FRIENDS OF THE PLEISTOCENE, ROCKY MOUNTAIN CELL, 45TH FIELD CONFERENCE

PLIO-PLEISTOCENE STRATIGRAPHY AND GEOMORPHOLOGY OF THE CENTRAL PART OF THE ALBUQUERQUE BASIN

FIRST-DAY ROAD LOG, OCTOBER 12, 2001

Geology of the Isleta Reservation

SEAN D. CONNELL
New Mexico Bureau of Geology and Mineral Resources-Albuquerque Office, New Mexico Institute of Mining and Technology, 2808 Central Ave. SE, Albuquerque, New Mexico 87106

DAVID W. LOVE
New Mexico Bureau of Geology and Mineral Resources, New Mexico Institute of Mining and Technology, 801 Leroy Place, Socorro, NM 87801

JOHN D. SORRELL
Tribal Hydrologist, Pueblo of Isleta, P.O. Box 1270, Isleta, NM 87022

The following road log examines some of the many outstanding geologic and geomorphic features on the Isleta Reservation. The first day of this field excursion examines lower Pleistocene deposits of the ancestral Rio Grande, the axial-river of the Albuquerque Basin and the namesake of the Rio Grande rift, and interfingering deposits of the eastern-margin piedmont. We also examine the role of faulting on the preservation of early Pleistocene and Pliocene geomorphic surfaces along the eastern margin of the basin. The day-one trip will conclude with a traverse to the eastern slopes of the late Pleistocene Cat Hills volcanic field to a visit to a graben on the San Clemente land grant. This graben preserves a sequence of sand and mud that overlies a buried soil developed on upper Pliocene fluvial deposits associated with rivers that drained the western margin of the basin. Many of the dates cited here are from Maldonado et al. (1999) and from unpublished data of Bill McIntosh and Nelia Dunbar (NM Bureau of Geology and Mineral Resources).

Nearly the entire following road log is on tribal lands administered by the Pueblo of Isleta, which are restricted to the public. Access to Pueblo lands must be made through the tribal administrator or governors office (Pueblo of Isleta, P.O. Box 1270, Isleta, New Mexico) prior to travelling on Pueblo lands. In respect for the privacy of the tribal community, we ask that you discuss access for geologic study or to access Pueblo lands to examine the exposures discussed herein with John Sorrell, Dave Love, or Sean Connell, prior to contacting the Governor's Office for permission. Road-log mileage has not been checked for accuracy. Field-trip stops illustrated on Plate I.

Mi.	Description
0.0	Begin trip at south side of store at the Isleta Lakes Campground, *Isleta 7.5' quadrangle (1991), GPS: NAD 83, UTM Zone 013 S, N: 3,867,855 m; E: 346,955 m. (Note that the UTM ticks on this quad are incorrect)*. Drive east and leave Isleta Lakes Campground. **0.3**
0.3	Railroad Crossing. **0.1**
0.4	Isleta Eagle Golf Course to south, a 27-hole course operated by the tribe and is part of their growing resort complex. **0.1**
0.5	Exposures of Arroyo Ojito Fm in bluffs to south. Basin-fill deposits are assigned to the upper Oligocene to lower Pleistocene Santa Fe Group, which comprises the synrift volcanic and sedimentary rocks of the Rio Grande rift. The Santa Fe Group is commonly subdivided into a lower subgroup representing deposition within internally drained (hydrologically closed) basins containing playa-lake, eolian, and piedmont deposits. Fluvial deposits from the proto-Rio Grande and Rio Puerco systems probably emptied into the northern and northwestern parts of the basin before these river systems integrated south into southern New Mexico during latest Miocene (?) or early Pliocene time. The upper sub-group represents deposition within externally drained (hydrologically open) basins where the Rio Grande represents the through-going axial river and contains a generally consistent pattern of lithofacies assemblages. Within externally drained half-graben basins, axial-fluvial deposits are bounded on either side by deposits derived from the footwall and hanging walls of the basin (Fig. 1-1). Hanging-wall deposits typically comprise the bulk of deposition, both spatially and areally. Axial-river deposits interfinger with piedmont deposits derived from rift-flank uplifts, such as the prominent chain of

mountains of the Sandia-Manzanita-Manzano-Los Pinos uplifts along the eastern rift border, and the Ladron Mountains to the southwest. In the Albuquerque area, upper Santa Fe Group deposits are three major lithofacies assemblages that represent distinctive depositional systems. The most abundant (both spatially and volumetrically) are deposits of the Arroyo Ojito Fm, which is a middle Miocene to Pliocene (and possibly earliest Pleistocene) fluvial succession associated with major western tributaries to the axial Rio Grande, such as the Rio Puerco, Rio Jemez/Guadalupe, and Rio San Jose systems (Fig. 1-2). These western rivers joined deposits of the ancestral Rio Grande just east of the present Rio Grande Valley during late Pliocene time. The present-day confluence of the Rio Puerco and Rio Grande is just south of Bernardo, New Mexico, about 55 km south of Isleta, New Mexico

Deposits of the axial-fluvial ancestral Rio Grande are provisionally assigned to the Sierra Ladrones Fm of Machette (1978) as are also locally derived deposits of the eastern margin that interfinger with these extrabasinal fluvial sediments. The Sierra Ladrones Fm has been extended from its type area at the southern edge of the basin, about 65 km to the south, by a number of workers (Hawley, 1978; Lucas et al., 1993; Smith et al., 2001), however, the stratigraphic and lithologic relationship between these deposits and those of the type area is ambiguous. The Sierra Ladrones Fm was defined without a type section and age control is generally poor in the type area. Studies of the type area of the Sierra Ladrones Fm (Connell et al., 2001a) are underway and results of this study should aid in its correlation throughout the basin. **0.1**

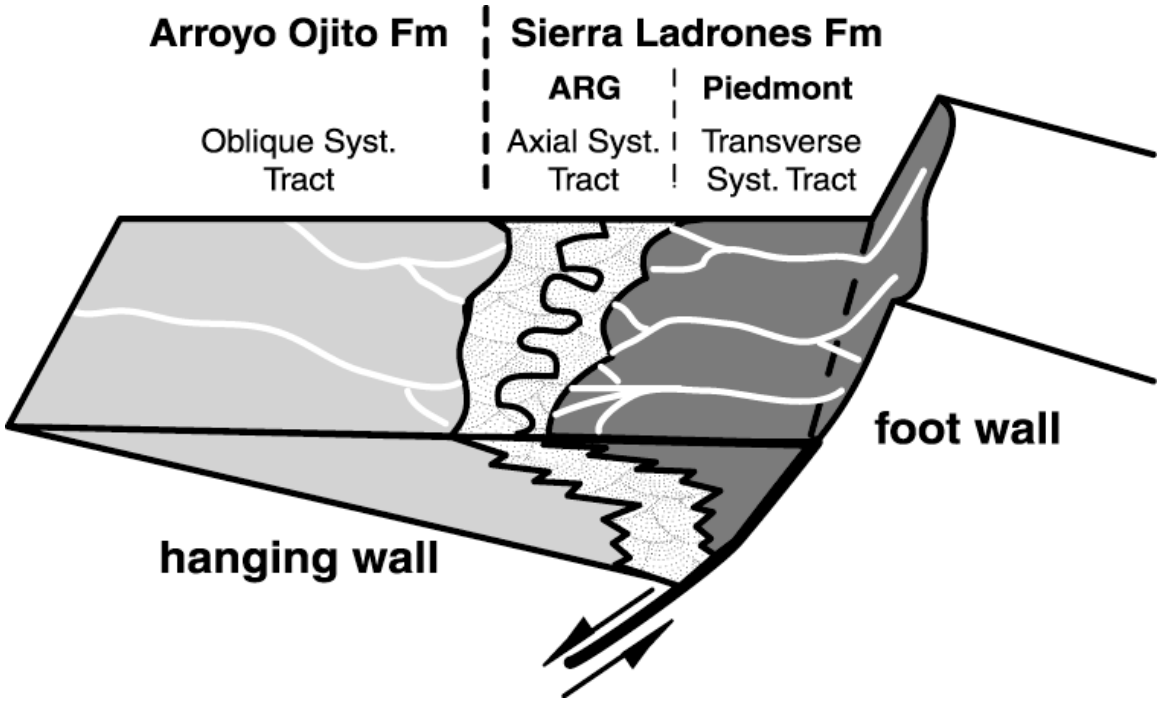

Figure 1-1. Diagram illustrating the distribution of sediments in a half-graben during deposition of the upper Santa Fe sub-Group (modified from Mack and Seager, 1990). This figure depicts the spatial distribution of major fluvial components. The axial-river is bounded on either side by deposits derived from the footwall and hanging wall of the half graben. This diagram represents a "post orogenic" stage of basin development where footwall-derived deposits prograde basinward during times of relative tectonic quiescence (see Blair and Bilodeau, 1988).

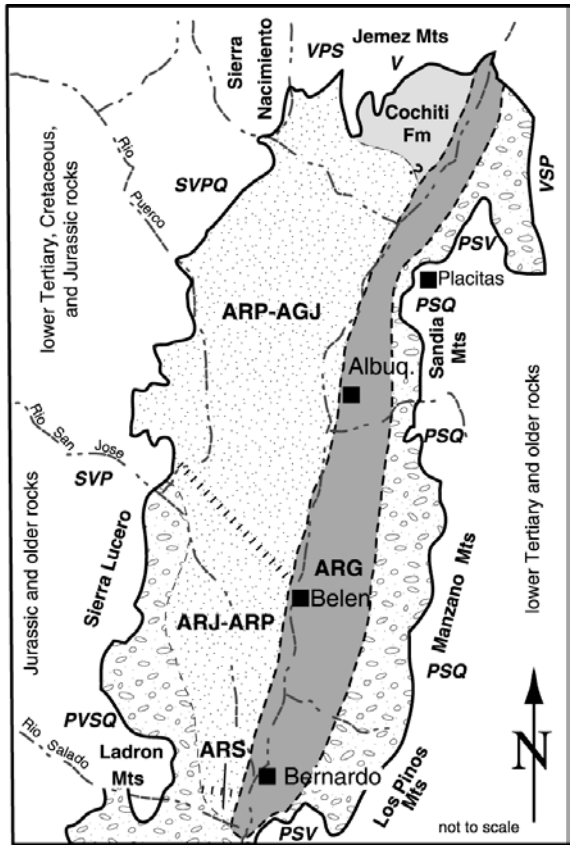

Figure 1-2. Schematic map showing the approximate areal distribution of major lithofacies in Pliocene sediments of the upper Santa Fe Group (modified from Connell et al., 1999; Love et al., 2001). The south-flowing ancestral Rio Grande (ARG) is the axial-fluvial facies (gray shading). The Arroyo Ojito Fm (stippled pattern) represents deposition by a series of large S-SE-flowing tributary drainages originating on the Colorado Plateau, San Juan Basin, Sierra Nacimiento, and western Jemez Mts. These deposits are associated with the ancestral Rio Puerco (ARP), Rio Guadalupe/Jemez (AGJ), ancestral Rio San Jose (ARJ), and ancestral Rio Salado (ARS). These fluvial deposits merge into a single axial-fluvial system at the southern margin of the basin. The conglomerate pattern delineates locally derived deposits from rift-margin uplifts. The Cochiti Fm (light-gray shading) consists of volcanic-bearing sediments shed off the southeast flank of the Jemez Mts. The boundaries among sub-drainages of the Arroyo Ojito Fm are approximate and diagrammatic. Sediment sources to deposits of the Albuquerque Basin include sedimentary and chert (S), volcanic (V), plutonic/metamorphic (P), and metaquartzite (Q).

0.7 Two normal faults with down-to-the-east displacement are exposed in Arroyo Ojito Fm to north on eastern edge of borrow pit. These faults are part of a wider zone included within the down-to-the-west Palace-Pipeline fault zone. This zone may be responsible for the presence of H_2S in groundwater in this area. **0.2**

0.9 Turn right (south) onto highway NM-47 at the Conoco Gas Station and Convenience Store. **0.1**

1.0 The upper Pliocene basaltic centers west of the Rio Grande Valley, include the 2.72-2.79 Ma Isleta volcano at 2:00, and the 4.01 Ma Wind Mesa volcano at 2:00-3:00 ($^{40}Ar/^{39}Ar$ dates summarized in Maldonado et al., 1999). Bluffs to the east are of the Arroyo Ojito Fm, overlain by a thin cap of ancestral Rio Grande deposits of the Sierra Ladrones Fm. The Arroyo Ojito Fm here contains base surge from Isleta volcano and fluvially recycled 2.75 Ma pumice. **0.2**

1.2 Cross arroyo. Fault exposed to your right cuts the Arroyo Ojito Fm and younger alluvium, locally. **0.2**

1.4 Milepost 40 and stop light. Isleta Casino and Resort to your left. **1.0**

2.4 Milepost 39. Arroyo Ojito Fm in road cuts ahead. **0.5**

2.9 Just west of the highway and near the level of the floodplain are exposures of the Arroyo Ojito Fm that contain fluvially recycled pumice dated at 2.68 Ma ($^{40}Ar/^{39}Ar$ date, W.C. McIntosh, unpubl.) and basaltic tephra (cinders) that were probably derived from 2.72-2.79 Ma Isleta volcano (Fig. 1-3). The contact between ancestral Rio Grande and western-fluvial deposits of the Arroyo Ojito Fm is unconformable here. At least 25-68 m of the underlying Arroyo Ojito Fm is missing here. **0.6**

3.5 Merge into left lane. **0.4**

3.9 Turn left (east) at stop light at intersection with NM-47 and SP-60/NM-147. Travel on Pueblo lands is restricted and permission must be obtained prior to entry. All tribal laws and customs must be obeyed on Pueblo lands. Permission to take photographs and samples must be obtained from tribal officials. Please drive slow (<10 MPH) through housing area. **0.4**

4.3 Cross cattle guard and ascend valley border. **0.5**

4.8 Exposures to south (right) are of the Isleta South Powerline stratigraphic section (Fig. 1-4). The uppermost gray beds are pumice-bearing deposits of the ancestral Rio Grande. Pumice pebbles and cobbles are fluvially recycled gravel of the Cerro Toledo Rhyolite (1.6-1.2 Ma) and Bandelier Tuff (1.2 and 1.6 Ma; Izett and Obradovich, 1994), which are early Pleistocene ignimbrite sheets that were emplaced during the development of the Jemez Mountains,

about 80 km to the north. These deposits also contain pebbles to small cobbles of black obsidian, which has been geochemically correlated to the 1.43-1.52 Ma Rabbit Mountain obsidian of the Cerro Toledo Rhyolite (Stix et al., 1988). These deposits are part of the axial-fluvial facies of the Sierra Ladrones Fm, which forms a 10-12-km wide axial ribbon that is typically exposed east of the present Rio Grande Valley. Deposits of the ancestral Rio Grande are recognized in drillholes within 2 km west of the front of the Sandia Mountains in the Northeast Heights section of Albuquerque and within 6 km of the Manzanita Mts. **0.3**

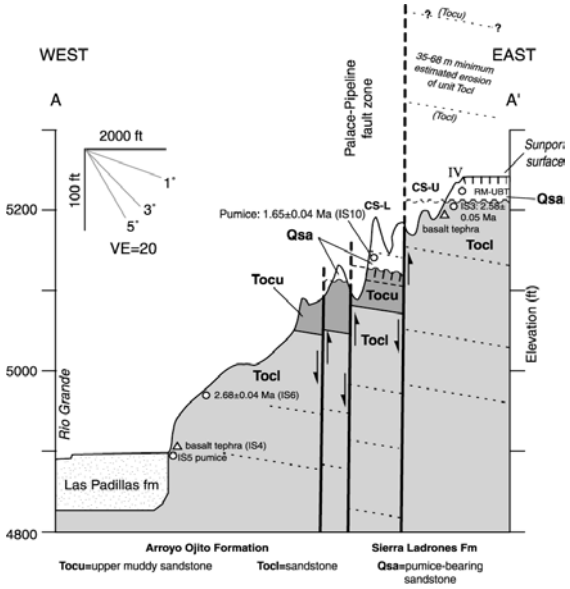

Figure 1-3. Cross Section of eastern bluff of Rio Grande Valley, illustrating age and stratigraphic relationships between the upper Arroyo Ojito Fm (Tocl, Tocu) and Sierra Ladrones Fm (Qsa). Unit Tocu contains abundant mudstone and overlies the sandstone dominated Tocl, which is similar to the Ceja Member of the Arroyo Ojito Fm. The amount of eroded and faulted section on the east (right) side of this cross section are based on estimates of the thickness of the sediment between the 2.68 Ma tephra and the highest preserved part of unit Tocu. Primary tephra indicated by open triangles, recycled pumice denoted by open circles. Hachures denote soils. Roman numerals indicate pedogenic carbonate morphologic stage. Dotted lines denote apparent dip of beds.

5.1 Turn right onto two-track dirt road. **0.2**

5.3 Intersection with two-track road. Continue straight. **0.1**

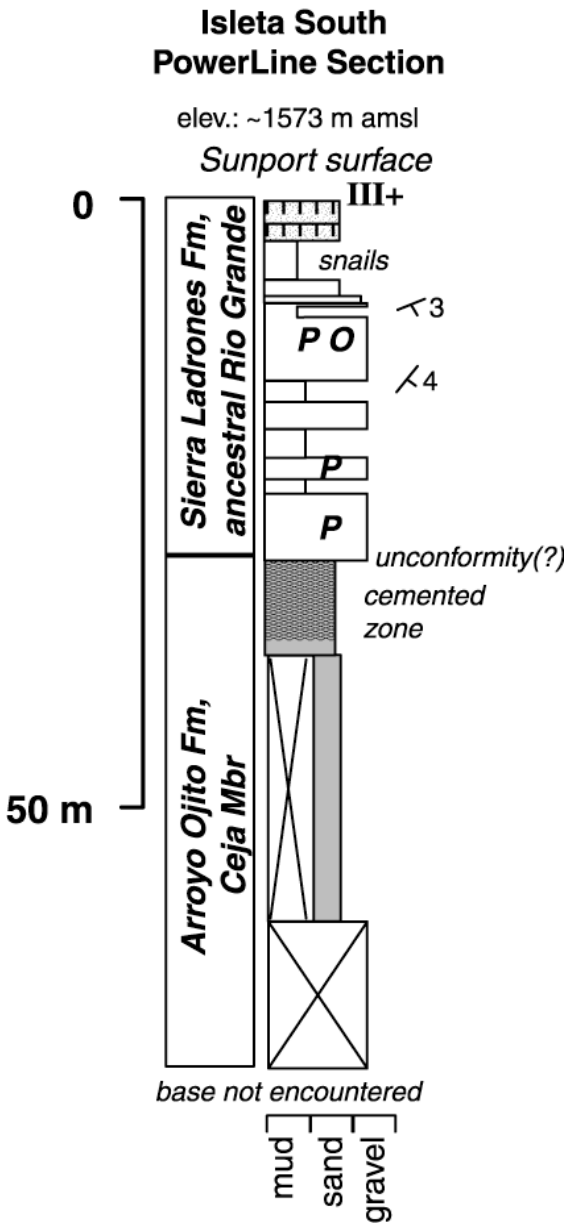

Figure 1-4. Stratigraphic column of the Isleta South Powerline composite section. Deposits of the ancestral Rio Grande contain fluvially recycled pumice (P) from the upper and lower Bandelier Tuff (BT) and Rabbit Mountain obsidian (O) of the Cerro Toledo Rhyolite. Fallout ashes and fluvially recycled pumice of the Cerro Toledo Rhyolite (1.55 Ma) and upper Bandelier Tuff (1.26 Ma, not shown here) are also found near the top of this section. These deposits overlie a moderately cemented and rhizoconcretionary-bearing interval in the Arroyo Ojito Formation, however, no distinctive unconformity is recognized here. Elsewhere, most notably near faults, this contact is unconformable. Bedding dips slightly to the southeast. Hachures denote soils. Roman numerals indicate pedogenic carbonate morphologic stage.

5.4 Ascend onto the Sunport surface, which is faulted by a number of down-to-the-west faults. The Sunport surface is a constructional surface named by Lambert (1968) for the Albuquerque International Airport (a.k.a. Sunport) on the north side of Tijeras Arroyo. This surface is part of the Llano de Manzano of Machette (1985). The Llano de Manzano was considered by Machette (1985) to represent a surface that graded to an alluvial terrace about 92-113 m above the modern Rio Grande. The Llano de Manzano is considerably lower than the Llano de Albuquerque surface to the west, which is about 110-215 m above the modern Rio Grande (Machette, 1985) and represents the upper constructional surface of the Arroyo Ojito Fm. Recent studies (Connell et al., 2000; Maldonado et al., 1999) indicate that the Llano de Manzano is composed of a number of different geomorphic surfaces, rather than a single surface. We use Lambert's (1968) Sunport surface to distinguish it from the slightly younger Llano de Manzano surface complex to the south and east, which contains piedmont deposits that prograde across much of this abandoned fluvial surface. We concur with Machette (1985) on the differences in age and geomorphic position between the Sunport/Llano de Manzano surfaces and the Llano de Albuquerque. Stratigraphic and geomorphic data suggest that the Sunport and Llano de Albuquerque surfaces are about two to five times older than estimated by Machette (1985). During Day 1 and 2 stops, we present evidence that the Sunport and Llano de Manzano surfaces should be considered part of the basin-fill succession, rather than as inset deposits that are stratigraphically disconnected from early depositional events.

The Sunport surface contains a petrocalcic soil that exhibits Stage III+ pedogenic carbonate morphology. Platy structure is locally recognized in natural exposures, but a laminar carbonate horizon is only weakly developed in places. On the basis of pedogenic carbonate development, Machette (1985) originally estimated the age of the Llano de Manzano surface to be about 300 ka. $^{40}Ar/^{39}Ar$ dates and geochemical correlations on tephra inset against and beneath the Sunport surface constrain the development of this constructional fluvial surface to between 1.2-0.7 Ma. **0.1**

5.5 **STOP 1-1.** East edge of Rio Grande Valley and ancestral Rio Grande deposits. Stop near trace of northeast-trending fault with down-to-the-west normal movement. *Isleta 7.5' quadrangle, GPS: NAD 83, UTM Zone 013 S, N: 3,864,180 m; E: 348,495 m*.

Light-gray, loose, sand and pebbly sand exposed just beneath the broad mesa of the Sunport surface are correlated to axial-river deposits of the ancestral Rio Grande, which is provisionally assigned to the Sierra Ladrones Fm. Gravelly intervals contain abundant rounded volcanic and metaquartzite cobbles and pebbles with minor granite. Chert is very sparse. Deposits of the ancestral Rio Grande unconformably overlie deposits of the Arroyo Ojito Fm along the eastern margin of the valley in the field-trip area (Fig. 1-4). Just north of this stop, this contact is slightly angular near a series of north-trending normal faults of the Palace-Pipeline fault zone exposed along the eastern margin of the Rio Grande Valley. Gravel contains scattered, fluvially recycled cobbles and rare boulders of the 1.22 Ma upper Bandelier Tuff. Fallout and fluvially reworked ashes are locally recognized in these deposits and have been dated and geochemically correlated to the 1.2 Ma Bandelier Tuff and the 1.55 Ma Cerro Toledo Rhyolite. Scattered rounded obsidian pebbles are also in this deposit. Some of these have been geochemically correlated to the 1.43-1.52 Ma Rabbit Mountain obsidian (Stix et al., 1988) of the Cerro Toledo Rhyolite. A mudstone containing aquatic and terrestrial gastropods is locally preserved between the loose sand and gravel and overlying fine-to medium-grained eolian sand and petrocalcic soil of the Sunport surface, which exhibits Stage III+ to locally weak Stage IV pedogenic carbonate morphology (Fig. 1-5). Cessation of deposition of the ancestral Rio Grande and development of the Sunport surface is constrained by deposits of the Lomatas Negras fm, which contains a fallout ash of the ~0.66 Ma Lava Creek B (Yellowstone National Park area, Wyoming and Montana). This terrace deposit is topographically lower than the Sunport surface, which contains a 1.26 Ma ash in Tijeras Arroyo. These stratigraphic and geomorphic relationships demonstrate that the Sunport surface developed between 0.7-1.2 Ma. This age is similar to ages of major erosional events reported for the abandonment of the lower La Mesa geomorphic surface and subsequent entrenchment of the Rio Grande in southern New Mexico (Mack et al., 1993, 1996), and for an unconformity between the St. David Fm and overlying alluvium in a tectonically quiescent basin in southeastern Arizona (Smith, 1994). The mudstone at the top of this section has been sampled for paleomagnetic studies by John Geissman (University of New Mexico) to better constrain the timing of development of the Sunport surface.

Figure 1-5. View looking north of Isleta South Powerline Section (Fig. 1-5) from footwall of northeast-trending normal fault. The white band at along the edge of exposures is the Sunport surface, which exhibits Stage III+ to locally weak Stage IV pedogenic carbonate morphology. Dave Love and 1.5-m scale on a snail-bearing mudstone bed preserved on hanging wall of unnamed northeast-trending fault. This mudstone pinches out at the left side of the photograph, near the lone juniper bush.

A major focus of this field trip is to document the timing late-stage filling of the Albuquerque Basin and subsequent entrenchment and development of smaller aggradational events associated with a long-term net decrease in local base level during Quaternary time. During aggradation of the Santa Fe Group, regional base level, as controlled by the Rio Grande, would have been increasing with a concomitant rise in groundwater levels (Fig. 1-6) and local development of phreatic cements. Using conceptual models of sedimentation in extensional basins (see summaries in Leeder and Jackson, 1993; Gawthorpe and Leeder, 2000), axial-fluvial sedimentation would be focussed along active eastern basin margin faults and rift-margin piedmont deposits would be limited to a rather narrow band near the eastern structural margin of the basin. The axial-fluvial system flowed longitudinally, whereas, hanging-wall deposits typically drained obliquely to the axial river. Deposits derived from the footwall flowed in a transverse orientation relative to the axial river. Concomitant deposition and tectonic subsidence along the basin-bounding fault would result in the development of interfingering and wedge-shaped stratal packages.

During entrenchment, the Rio Grande Valley formed in a series of episodic entrenchment and partial aggradation events. This net decline in base level would result in the removal of water in the aquifer. Deposits associated with the development of incised valleys contain somewhat tabular fluvial successions of extrabasinal detritus. The margins of these deposits are bounded by locally derived alluvium from bluffs. These deposits have bounding disconformities along the base and margins. In particular, the margins of such deposits are distinctive in their development of buttress unconformities, which include buried paleobluffs.

A recent model of late-stage basin sedimentation and entrenchment, based upon the work of Machette (1985) and Reneau and Dethier (1996), was proposed by Cole (2001a, b) and Stone (2001a, b). This, termed herein as the Cole-Stone (CS) model for convenience, proposes that widespread aggradation of synrift basin filling ceased during late Pliocene time, by about 2.5 Ma, when the ancestral Rio Grande entrenched into older deposits of the upper Santa Fe Group. They proposed that this late Pliocene entrenchment created the constructional surface of the Llano de Albuquerque, the interfluve between the valleys of the Rio Puerco and Rio Grande.

The CS model agrees with Machette's (1985) interpretation of the early Pleistocene deposits of the Sunport surface representing the oldest inset fluvial terrace deposit in the basin (Stone et al., 2001a,b). This inset relationship is based on inferences regarding the location of the paleo-groundwater table using the spatial and temporal distributions of phreatomagmatic and non-phreatomagmatic eruptions in the region (Cole et al., 2001a), and in a record of repeated entrenchment and aggradation events dating back to early Pliocene time in White Rock Canyon (Reneau and Dethier, 1996) at the margin of the Española and Albuquerque basins, about 80 km to the north (Fig. 1-7).

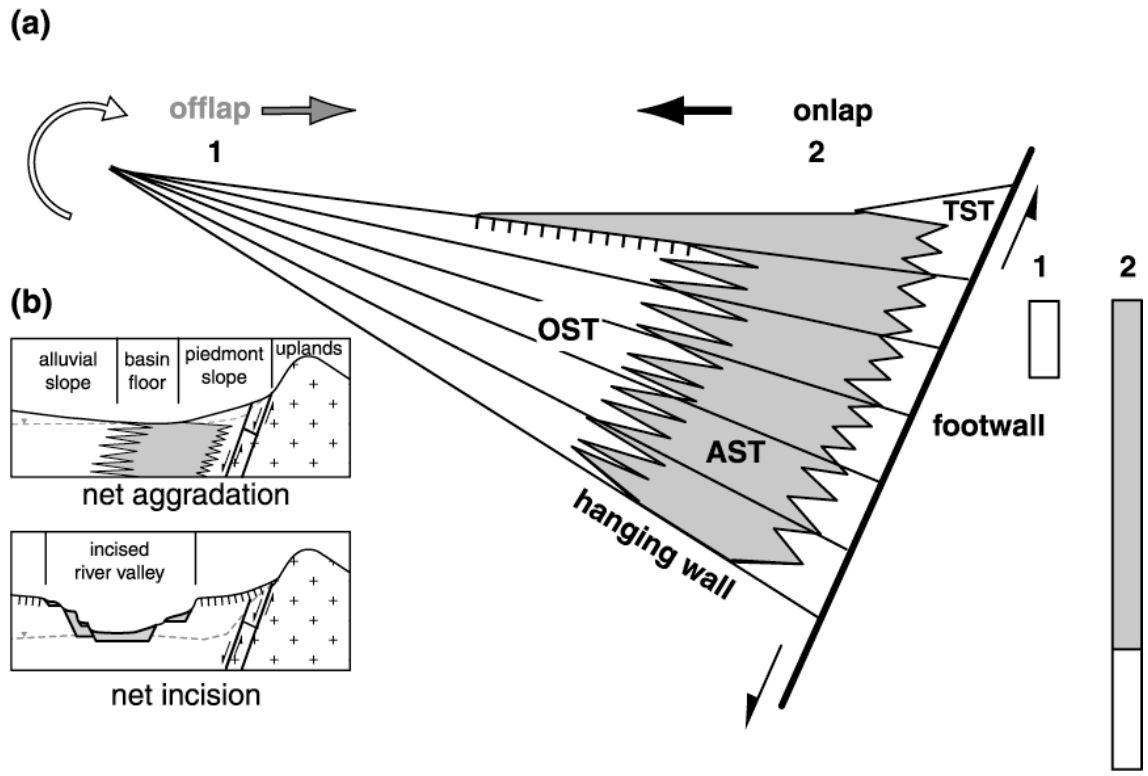

Figure 1-6. Hypothetical stratigraphic relationships of sedimentation in an actively subsiding half-graben basin; intrabasinal faulting is not accounted for in this conceptual model. Intrabasinal faults can create local fault-wedge stratigraphic successions that would have similar stratal geometries to this model; however, deposition would be dominated by eolian and colluvial processes, rather than fluvial. Deposits from the hanging wall (Oblique systems tract; Arroyo Ojito Fm) are volumetrically the largest component of the basin fill. The axial-fluvial system (AST) occupies the central part of the basin and interfingers with OST and locally derived transverse deposits (TST) from the footwall uplift. During times of significant footwall upflift (or basin subsidence), AST and TST will be close to the uplifting footwall block (*cf.* Blair and Bilodeau, 1988). During times of relative tectonic quiescence or slower subsidence rates, TST will onlap onto AST and AST will onlap onto OST (*cf.* Blair and Bilodeau, 1988; Mack and Seager, 1990). Offlap and the development of sediment bypass surfaces on the OST could occur along the hanging-wall border because of the relative lack of space developed in this simple block rotational model. If the OST has been abandoned, then an unconformity between AST and OST will develop during westward onlap of AST onto older OST deposits as AST and TST progrades basinward. This interaction between deposition and subsidence in this simplified fault block results in the development of wedge-shaped stratal units and eastward thickening from the up-dip portion of the hanging wall (1) and the continually subsiding footwall (2). Offlap of the western-fluvial facies could occur as progressive rotation of the hanging wall creates subsidence along the footwall. This would likely result in the development of unconformities along the up-dip portions of the hanging wall. Progradation of axial-river and piedmont deposits could occur during onlap of these deposits onto the hanging wall surface of western-fluvial deposits, resulting in the development of a wedge of axial-river and piedmont deposits near the footwall. The hachured area denotes the development of an unconformity along the boundary between western fluvial deposits (oblique depositional systems tract, OST), and the axial-fluvial systems tract (AST) of the ancestral Rio Grande. Westward onlap of the AST would result in the preservation of an unconformity that would increase in magnitude towards the up-dip portion of the hanging wall. Continued deposition between the AST and the eastern piedmont (transverse systems tract, TST) would occur towards the footwall. B) Hypothetical diagram contrasting deposition in an aggrading basin (i.e., Santa Fe Group time) and episodic deposition during periods of long-term net entrenchment. During net aggradation, base level rises and facies interfinger with one another and deposits tend to have a wedge-shaped geometry and thicken towards the basin-bounding fault. During net entrenchment, base level fall and the upper parts of the basin fill system are drained of water. Episodic aggradational events are recorded as unconformity bounded tabular sedimentary units. Progressive net decline in base level and groundwater levels, which drained out of the upper part of the basin-fill aquifer. Dashed lines represent paleo-base level positions of the axial river.

Basic elements, either explicitly required, or reasonably inferred by the CS model include:

- Development of phreatomagmatic volcanism during aggradational phase of basin because of near surface groundwater.
- Lack of thick or extensive fluvial deposits during a nearly 2 m.y. interval, between about 2.8-0.8 Ma. An exception is along the La Bajada fault zone, which defines the Albuquerque- Española basin boundary.
- Widespread hiatus in deposition indicates that the drainage system had begun to erode into upper Santa Fe Group strata by 2.5 Ma.
- Oldest significant post-phreatomagmatic-basalt fluvial deposits are preserved as a terrace east of the Rio Grande Valley.

The model proposed by Connell et al. (2000; 2001c) and Love et al. (2001) and modified herein, suggests that:

- Basin-fill aggradation occurred during Pliocene and Pleistocene changes in climate. Stratigraphic and subsurface studies (Connell et al., 1998a, 1999; Hawley et al., 1995) note that deposits become markedly coarser near the top of the Santa Fe Group. Incision of the Santa Fe Group occurred between 0.7-1.2 Ma here. This bracketed age is similar to well documented entrenchment events in the Camp Rice Fm (southern New Mexico correlative of the Sierra Ladrones Fm), suggesting that entrenchment was of a regional nature.
- Late-stage deposition of the Santa Fe Group was strongly controlled by the activity and location of intrabasinal faults. This tectonic influence on sedimentation would be increased if sedimentation rates were slow, too.
- Determination "normal" aggradational stratigraphic successions vs. incised fluvial-terrace suites can be difficult, especially in the Albuquerque Basin, where most of the basin-fill and post-basin-fill deposits are lithologically similar. However, stratal geometries and unconformity development can be useful tools in discriminating between these two different depositional processes.

Landscape evolution can be inferred by reconstructing pre-faulting positions, ages, and stratigraphic-geomorphic setting of volcanic deposits, which are useful because they are resistant to erosion and have reasonably predictable surface forms. In particular, topographic inversion of basaltic flows are useful in determining the rate and magnitude of valley entrenchment. However, care must be used when inferring paleo-groundwater conditions because phreatomagmatic eruptions could occur where perched groundwater is present. Volcanic features bury and preserve paleo-topography, however, the relative stability a particular paleo-topographic surface (i.e., stable geomorphic surface, or just a preserved bed in an otherwise conformable stratigraphic sequence) can only be deduced with confidence where indicators of surface stability, such as soils, are present.

Rates of Plio-Pleistocene fluvial deposition are poorly constrained by are on the order of about 100 m/m.y. or less near San Felipe Pueblo (Derrick and Connell, unpubl. data). This rate is significantly slower than rates of deposition of the Popotosa Fm (lower Santa Fe sub-Group), which were near 400 m/m.y. during late Miocene time (Lozinsky, 1994). Thus, rates of deposition slowed by Pliocene time, but deposition was occurring in the basin (see Smith et al., 2001).

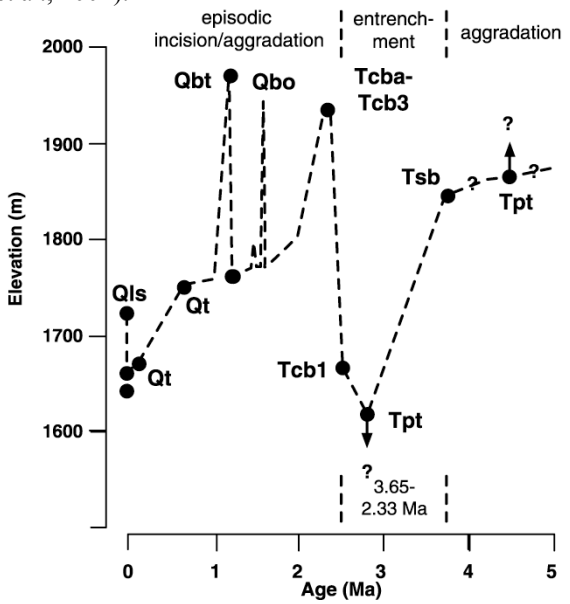

Figure 1-7. Graph depicting timing of major entrenchment and aggradation events in the southern Española Basin at White Rock Canyon (Reneau and Dethier, 1996), about 85 km north of Stop 1-1. The black circles represent dated deposits and the projected position of the ancestral Rio Grande. The dashed line represents projected levels of the ancestral Rio Grande through time in White Rock Canyon, which is on the footwall of the La Bajada fault and has been strongly affected by repeated Plio-Pleistocene volcanic events. Refer to Reneau and Dethier (1996) for discussion of methods and dates. Deep incision occurred between about 3.65-2.33 Ma in White Rock Canyon. This was followed by repeated aggradation and deep incision events throughout late Pliocene and Pleistocene time. Note that the Rio Grande was aggraded to 1970 m)and above its former position prior to ~3 Ma) after 1.2 Ma and before White Rock Canyon was entrenched.

In the Española Basin, Reneau and Dethier (1996) provide excellent evidence for repeated Pliocene and Pleistocene entrenchment events that may be related to climatically and geomorphically (e.g., volcanically and tectonically) driven incision. Their study area is near the structural margin of the Española and Albuquerque basins and lies within a geomorphically, volcanically, and tectonically active area, where deposition and incision were strongly influenced by faulting and episodic damming of the river valley. Here at Isleta, local unconformities are interpreted as the result of concurrent deposition and tilting (Connell et al., 2001b) and local uplift of an intrabasinal horst (Love et al., 2001). We suggest that these apparently disparate controls on sedimentation influence the depositional system in different, but not mutually exclusive, manners. For instance, deposits of the upper Santa Fe Group generally coarsen upwards (see Connell et al., 1998b). The development of these coarsening upwards sequences in the uppermost Santa Fe Group demonstrate increased competence of Plio-Pleistocene rivers and could be associated with an increase in effective moisture during Plio-Pleistocene times; however, coarsening of piedmont deposits could also be attributed to basinward progradation during times of tectonic quiescence (Leeder and Gawthorpe, 1987; Blair and Bilodeau, 1988).

The CS model differs from part of the model of Connell et al. (2000, 2001c), which suggests that spatially time-transgressive sedimentation and development of local stratigraphic tops in the Santa Fe Group occurred into Pleistocene time. This diachroneity of sedimentation is strongly influenced by continued faulting and tilting in the basin during late Pliocene and Pleistocene time, which resulted in the development of unconformities on the up-dip portions of hanging wall blocks and concomitant aggradation near basin depocenters (Connell et al., 2001c). The presence of numerous scarps cutting Pleistocene deposits attests to continued deformation within the basin. This is supported by paleoseismic studies of the basin that indicate Quaternary movement of intrabasinal faults between 2-20 m/m.y. (Machette et al., 1998; Personius et al., 1999; Personius, 1999; Wong et al., *in prep*).

The CS model proposes that the Sunport surface represents the highest inset fluvial terrace deposit in the Albuquerque Basin (Stone et al., 2001a,b). If this interpretation is true, then this rather broad (5-10 km wide) terrace deposit should be inset against older basin fill deposits along the eastern margin. Geologic mapping of the Isleta Reservation to the northeastern edge of the basin (Cather and Connell, 1998; Cather et al., 2001; Connell and Wells, 1999; Maldonado et al., 1999; Smith et al., 2001) does not recognize such a buttress unconformity. Instead deposits of the ancestral Rio Grande system interfinger with deposits shed off of eastern margin uplifts and are buried by progradation of eastern-margin piedmont detritus.

Stratigraphic evidence along strands of the Hubbell Spring fault zone shows early Pleistocene deposits of the ancestral Rio Grande are an integral part of the basin-fill depositional system in an asymmetric or complexly faulted half-graben basin. We argue that deposition of the Santa Fe Group generally ceased when the Rio Grande unequivocally entrenched into older fluvial deposits during early Pleistocene time, forming discontinuous flights of unpaired terrace deposits that border the Rio Grande Valley. Deposition of the Santa Fe group continued locally into the Pleistocene, where smaller non-integrated drainages deposited sediment onto broad abandoned plains and piedmont-slopes of the Llano de Manzano. Intrabasinal faulting and coeval sedimentation resulted in the formation of a number of distinct geomorphic surfaces on local uplifted fault blocks, resulting in the development of a number of local tops of the basin fill. South of the Española Basin, many workers generally consider the Santa Fe Group basin-fill system to have aggraded until early Pleistocene time, when the Rio Grande Valley formed (Smith et al., 2001; Connell and Wells, 1999; Connell et al., 1998; Maldonado et al., 1999; Hawley et al., 1995).

Our interpretation of the stratigraphy has the distinct advantage of distinguishing basin-fill from younger entrenched deposits with less ambiguity that the C-S model. The determination of hiatal surfaces along the eastern margin of the basin would be difficult, mainly because of the influence of faulting on sedimentation and because age control is generally lacking for much of the sedimentary succession. Along the eastern margin of the Albuquerque Basin, between Cochiti Pueblo and Hell Canyon Wash, exposures and drillhole data indicate the presence of conformable stratigraphic successions of Plio-Pleistocene age. The presence of soils locally marks unconformities or hiatuses in the section. However, these would be rather difficult to extend across a tectonically active basin. By picking a broader set of criteria for basin-fill aggradation, these ambiguities are diminished, especially in areas with little subsurface control or exposure.

Problems with reconciling these two models is important because the CS model requires the presence of a rather profound unconformity beneath the eastern side of the basin to accommodate their Sunport terrace. The removal of over 70 m of Pliocene sediment would create a previously unrecognized major hydrogeologic discontinuity in Albuquerque's aquifer. The presence of such a discontinuity would also significantly revise estimates of the amount of drawdown required for irreversible subsidence, as was recently estimated by Haneberg (1999).

Stratigraphic evidence amassed by Sean Connell and Dave Love since 1997, indicates the presence of an intraformational unconformity between early Pleistocene deposits of the ancestral Rio Grande and the Arroyo Ojito Formation on Isleta Pueblo and Tijeras Arroyo. To the south, the unconformity between the Sierra Ladrones and Arroyo Ojito formations diminishes. A major unconformity within the ancestral Rio Grande is recognized locally between deposits containing the Cerro Toledo ash and overlying coarse gravels of the Rio Grande north of the mouth of Hell Canyon Wash (see Day 2). This unconformity is related to local faulting and migration of the ancestral Rio Grande. This unconformity may die out to the east. Such unconformable relationships are recognized in a few areas, and thus may not be applicable in a regionally consistent manner without precise age constraints.

Turn vehicles around and drive towards SP-60. **0.3**

5.8 Hard right onto east-trending two-track road, which rejoins SP-60 heading east. **0.2**

6.0 Turn east onto SP-60. **0.4**

6.4 Ascend scarp of Palace-Pipeline fault, which cuts deposits of the ancestral Rio Grande. The trace of the Palace-Pipeline fault, which is about 19-m high here, is named for its proximity to the old Isleta Gaming Palace and a gas pipeline. This fault roughly corresponds with the location of the Rio Grande fault of Russell and Snelson (1994) south of Albuquerque. Russell and Snelson (1994) proposed the Rio Grande fault as a prominent intrabasinal normal fault that cut off the range-bounding normal faults of the Manzanita and Sandia Mountains after late Miocene or Pliocene time (Russell and Snelson, 1994). Russell and Snelson (1994) projected their Rio Grande fault northward and beneath the inner valley. Their Rio Grande fault was projected beneath downtown Albuquerque, New Mexico, and extended north to Bernalillo, New Mexico. Russell and Snelson (1994) proposed this projection on the basis of drillhole data on the Isleta Reservation and on two partial lines of seismic reflection data and drillhole data that demonstrate the presence of a major intrabasinal graben beneath the present Rio Grande Valley (Fig. 1-8). Gravity data (Grauch et al., 1999) and geologic studies of the basin (Maldonado et al., 1999; Connell and Wells, 1999; Connell et al., 1998) suggest that this intrabasinal structure is likely an older feature that probably trended to the northwest rather than to the north (Maldonado et al., 1999). The presence of thick early Pleistocene deposits on the footwall of the Rio Grande fault does not support the presence of significant Pleistocene activity along this fault. However, the presence of an unconformity and intrabasinal faults exposed along the eastern margin of the Rio Grande Valley at Stop 1 does support significant late(?) Pliocene tectonism near the present day valley. **0.2**

6.6 Cross cattle guard and descend broad east-tilted footwall block of Palace-Pipeline fault. This block generally slopes towards west-facing scarps of splays between the Palace-Pipeline fault and the McCormick Ranch fault zone. The TransOcean Isleta #1 well, about 1.8 km to the north, was drilled to 3163 m below land surface (bls) and encountered 1563 m of Santa Fe Group basin fill (Fig. 1-8; Lozinsky, 1994). The Shell Isleta #2 well, drilled just west of Isleta volcano, was drilled to 6482 m bls and encountered 4407 m of Santa Fe Group strata (Lozinsky, 1994). **0.6**

7.2 Borrow pit on north side of road exposed strongly developed petrocalcic soil of the Sunport surface, which exhibits Stage III+ carbonate morphology. This soil is overlain by eolian sand that contains weakly developed buried soils (Fig. 1-9). **0.3**

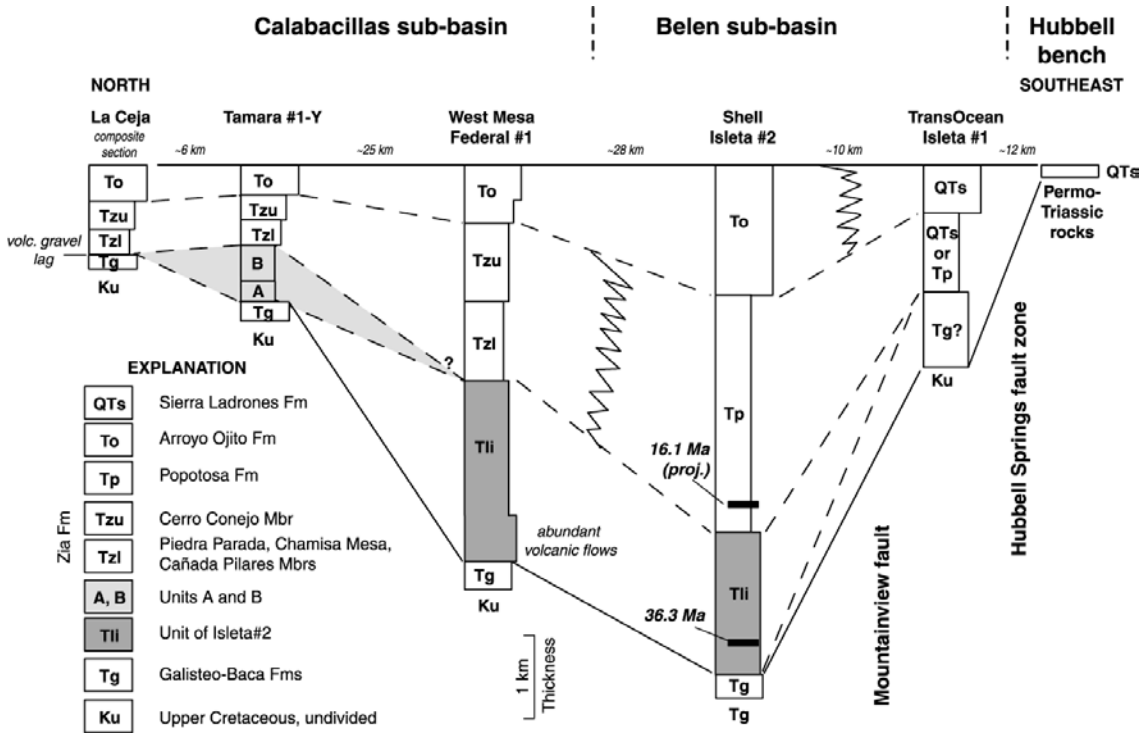

Figure 1-8. Stratigraphic fence of Cenozoic deposits in the Calabacillas and northern Belen sub-basins. Data from oil test wells (Lozinsky, 1988, 1994; Connell et al., 1999; Tedford and Barghoorn, 1999; Maldonado et al., 1999; Black and Hiss, 1974). From Connell, Koning, and Derrick (2001).

Figure 1-9. Photograph of petrocalcic soil of the Sunport surface, exhibiting Stage III+ pedogenic carbonate morphology overlain by fine- to medium-grained sand of eolian origin. The overlying eolian sand commonly forms an extensive cover over the carbonate of the Sunport surface. Scale is 1.5 m.

7.5 Cross west-facing scarp of fault cutting ancestral Rio Grande deposits that are overlain by a thin veneer of eolian sand. **0.4**

7.9 Cross west-facing scarp of fault cutting ancestral Rio Grande deposits. Descend east-sloping footwall dip slope. **0.5**

8.4 Cross west-facing scarp of fault cutting ancestral Rio Grande deposits. **0.1**

8.5 Descend into unnamed northern tributary valley to Hell Canyon Wash. Prominent bench ahead just west of the front of the Manzanita Mountains is the northern Hubbell bench, which exposes Permo-Triassic rocks and thin well cemented conglomerate and sandstone of older Santa Fe Group deposits. **0.4**

8.9 Tributary valley of Hell Canyon Wash. **0.3**

9.2 On east-facing scarp of down-to-the-east McCormick Ranch fault. **0.3**

9.5 Near western pinchout of piedmont deposits, which overlie ancestral Rio Grande deposits here. Note that gravel is typically subrounded to angular and composed of limestone, quartzite, schist, and granite. **0.2**

9.7 Road is on terrace of Memorial Draw, a tributary to Hell Canyon Wash. It is named for a small memorial erected by the parents of one of several Navy fliers killed in a crash here in 1946. This terrace is buried by Holocene alluvium upstream and was removed by erosion downstream. Higher terraces are cut by strands of the Hubbell Spring fault zone. **0.6**

10.3 Cross gas pipeline. **0.7**

11.0 Cross cattle guard. Large cottonwood at 11:00 is Hubbell Spring, on the eastern strand of the Hubbell Spring fault zone. The

Hubbell Spring fault zone is subdivided into three major strands (Maldonado et al., 1999; Personius et al., 1999). The eastern strand forms the embayed escarpment of the Hubbell bench and juxtaposes reddish-brown Permo-Triassic sandstone and mudstone against deposits of the Santa Fe Group. The central and western strands of the Hubbell Spring fault zone commonly have prominent scarps and are geomorphically young and have rather distinct linear traces. Note the large Cottonwood at 1:00, which is on the central strand of Hubbell Spring fault zone and is the location of Stop 2-2. **0.4**

11.4 Pass intersection with road to Hubbell Spring to left. **0.6**

12.0 Pull off road. **STOP 1-2. Hubbell Spring fault zone.** *Hubbell Spring 7.5' quadrangle, GPS: NAD 83, UTM Zone 013 S, N: 3,865,030 m; E: 358,090 m.*

At this stop we examine some spring deposits on the footwall of the central strand of Hubbell Spring fault zone, tectonic controls on groundwater and sedimentation, and paleoseismicity of the Hubbell Spring fault zone. Wells on south side of road encounter water at about 6 m below land surface. A deeper groundwater monitoring well (28D), drilled about 25 m north of the road, exhibits decreasing water levels with depth, indicating that this is a groundwater recharge area associated with this fault (Fig. 1-10). The high level of groundwater is also indicated by the presence of the large Cottonwood on the hanging wall of this fault strand. There are two prominent springs associated with this strand of the Hubbell Spring fault zone. Hubbell Spring and Ojo de la Cabra (Goat Spring) are about 2.5 km north and south of this stop. Deposits encountered in well 28D indicate that fluvial deposits of the ancestral Rio Grande interfinger with limestone-bearing piedmont deposits derived from the front of the Manzanita Mountains. The presence of fluvial deposits of the ancestral Rio Grande is supported by observations of similar strata exposed in a trench on the footwall of the central Hubbell Spring fault zone to the north (Personius et al., 2000). This well bottomed in limestone that we interpret to represent conglomerate from the piedmont member of the Sierra Ladrones Fm, rather than from the Madera Group, which would be much lower in the stratigraphic section, and below Paleogene-Triassic red beds, which were not encountered in cuttings sampled from this well. If this limestone interval is the Pennsylvanian Madera limestone, it then requires that about 580 m of Permo-Triassic rocks (estimated from eastern slope of Sandia Mountains; Ferguson, 1996) be missing from the drillhole section. This interpretation would suggest the presence of reverse faulting, probably of Laramide age; however, the presence of Permo-Triassic strata on the footwall of the eastern strand of the Hubbell Spring fault zone does not support this interpretation. Also, the presence of dark-gray Paleocene mudstone in wells on the Isleta-Sandia National Labs boundary (Thomas et al., 1995) indicate fine-grained, low energy deposition during early Cenozoic time. Another possible explanation is that the limestone was deposited by streams draining the western front of the Manzanita Mts. Pennsylvanian limestone is well exposed along the eastern basin margin and is also exposed on the footwall of the eastern Hubbell Spring fault on the lands of the Sandia National Laboratories and Kirtland Air Force Base, which abuts the northern boundary of the Isleta Reservation.

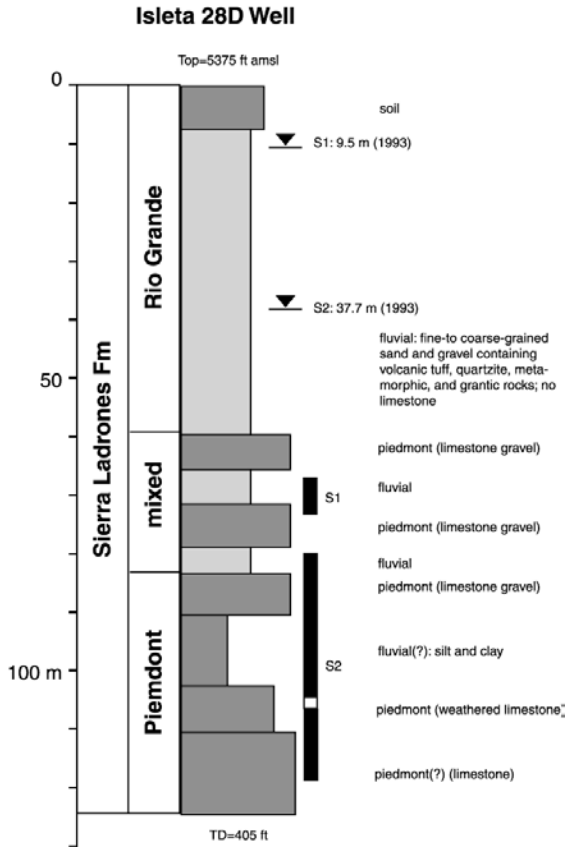

Figure 1-10. Stratigraphic column of monitoring well MW28D drillhole and stratigraphic interpretations. The black rectangles depict upper (S1) and lower (S2) screens, which have associated water levels of 9.5 m and 37.7 m bls, respectively.

The presence of ancestral Rio Grande deposits less than 2 km west of the Hubbell bench, which is underlain Permo-Triassic red beds indicates that the Rio Grande was at least 12 km east of its present course. Geologic mapping of the region and stratigraphic studies within the two largest tributary canyons to the Rio Grande, Hell Canyon Wash and Tijeras Arroyo, do not support the presence of a

buttress unconformity or paleobluff line between early Pleistocene deposits of the ancestral Rio Grande and eastern-margin piedmont deposits. Instead the stratigraphic relationships in these arroyos suggests an interfingering relationship between the axial-fluvial and transverse piedmont system, as recognized in elsewhere in Plio-Pleistocene basin-fill systems, such as the Palomas Fm of southern New Mexico (Mack and Seager, 1990; Gile et al., 1981). In contrast, the CS model implies the presence of a major stratal discontinuity along the eastern basin margin that would juxtapose early Pleistocene deposits against older (Pliocene) strata. Intrabasinal normal faults could act as this unconformable boundary; however, the presence of ancestral Rio Grande deposits across traces of the central Hubbell Spring fault suggests that this fault strand does not exert enough control over the eastern limit of the axial-fluvial system during late Pliocene(?) time. The stratigraphic relationship in MW28D indicates structural control on the stratigraphic position of ancestral Rio Grande deposits, however, the relative lack of reworked extrabasinal detritus in the piedmont section suggests that faulting did not produce a significant escarpment during Plio-Pleistocene deposition.

One of the younger strands of the Hubbell Spring fault zone was studied by Steve Personius of the U.S. Geological Survey in the fall of 1997 (Personius et al., 2000). A trench was excavated on the steepest, most youthful looking fault scarp near the northern end of this fault zone, about 2 km to the north of this stop (Figs. 1-11 and 1-12). Seven stratigraphic units were described in the excavation. These deposits consist of a lower light-gray fluvial deposit (unit 1) that is overlain by locally derived alluvial deposits (unit 2). These are overlain by a series of eolian and alluvial deposits (3-8). The lowest deposit was recognized as fluvial and correlated with the early Pleistocene Santa Fe Group (Personius et al., 2000), however, provenance of this deposit was not indicated. These deposits contain rounded volcanic and metaquartzite pebbles having a strong affinity to ancestral Rio Grande deposits, which were also recognized on the footwall of this strand of the Hubbell Spring fault at monitoring well MW28D. Soils described on alluvium on the far-field part of the footwall block indicate the development of Stage IV pedogenic carbonate morphology (Personius et al., 2000). The younger eolian sediments of units 4, 5, and 7 are composed of eolian sand and were dated using thermoluminescence (TL) and infra-red stimulated luminescence (IRSL) methods at 52-60 ka, 27-34 ka, and 11-14 ka , respectively (Personius et al., 2000). Unit 5 is offset by the fault and unit 9 buries the fault. Stratigraphic relationships of units 6-8 relative to the fault are not apparent. The older alluvial deposits were dated using Uranium-series disequilibrium methods and yielded ages ranging from 70-244 ka, with the best date of 92±7 ka (Personius et al., 2000) for a trench containing the Stage IV carbonate soil on the footwall. Interpretation of the fault-rupture history for this strand of the Hubbell Spring fault indicate three episodes of movement during late Pleistocene time (Fig. 1-13). The latest event is estimated to have occurred during latest Pleistocene time.

Slip-rate estimates for basin-margin faults that cut across the seismogenic crust are on the order of 0.02-0.2 mm/yr (20-200 m/m.y.). Slip-rate estimates for intrabasinal faults in the Albuquerque area are on the order of 0.004-0.05 mm/yr (4-50 m/m.y.) (Personius, 1999). Estimated recurrence intervals for basin-margin and intrabasinal faults are 10-50 ka and 10-200 ka, respectively (Personius, 1999). Thus, faulting of the 0.7-1.2 Ma Sunport surface would result in between 3-60 m of movement across intrabasinal faults.

East and southeast of the water tank at Stop 1-2 are low hills interpreted to be former spring mounds. At the surface of these mounds and in interbedded alluvial and eolian deposits are layers of fragmented plates and nodules of micritic calcium-carbonate sandstone. One such spring mound is exposed along the footwall of the Hubbell Spring fault on the north side of the road (Fig. 1-14). This exposure has a sharp base with underlying uncemented sand. Other exposures of spring deposits have sharp bases and large masses of oxidized and hydrated iron and manganese stain deposits red, orange, yellow, and black. In reduced environments, reduced iron, and stains sediments green, gray, and black. These deposits commonly contain root molds or casts and represent precipitation in poorly drained sediment, such as those along springs. These features differ from more common pedogenic features that are typical of the well-drained semi-arid soils. Features common in well-drained, semi-arid soils include distinctive horizonization, and a gradual downward decrease in calcium-carbonate cement and soil structure. Exceptions to these morphologic differences can occur across major textural boundaries. Also, spring and pedogenic carbonates may be reworked or superimposed along fault zones or major escarpments, such as along the edges of the Cañada Colorada surface to the east. (Fig. 1-15).

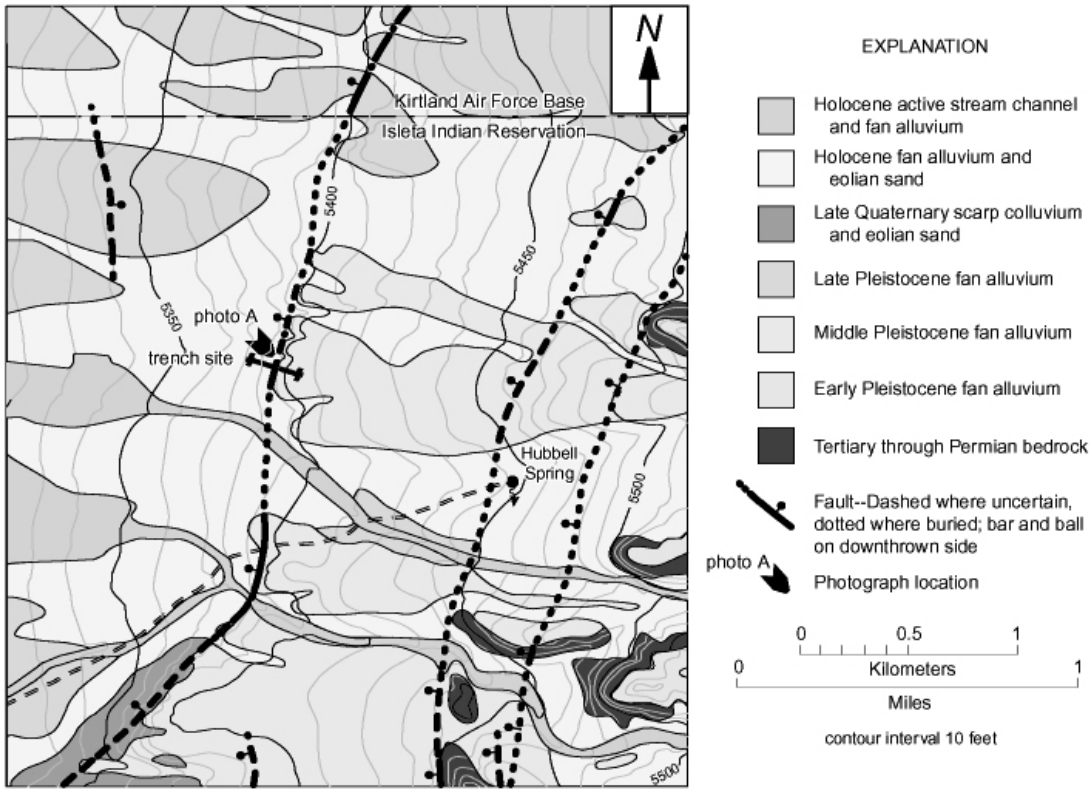

Figure 1-11. Geologic map of trench site area, northern Hubbell Spring fault zone (Personius et al., 2000). The trench site is about 2 km north of stop 1-2.

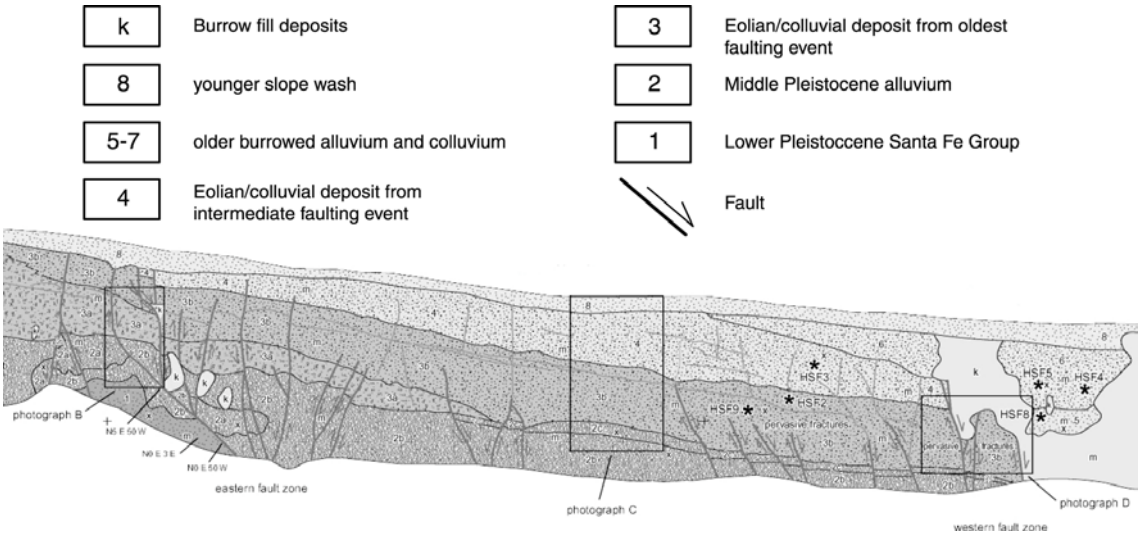

Figure 1-12. Part of paleoseismic trench across central strand of the Hubbell Spring fault zone (Personius et al., 2000), illustrating displacements of units 1-4.

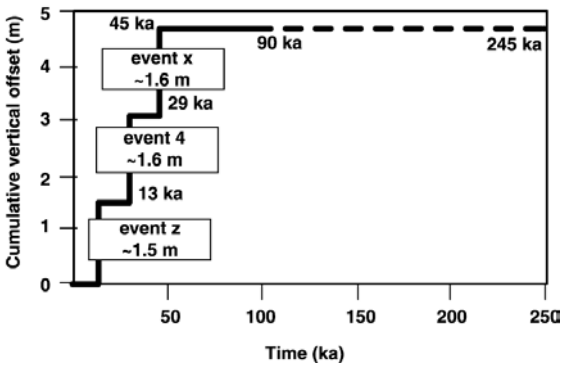

Figure 1-13. Time-displacement diagram for the Hubbell Spring fault zone (Personius, 1999). The two oldest dates are U-series ages on calcic soil rinds developed on alluvial gravels that predate the oldest event. The younger dates are based on thermoluminescence (TL) ages on sandy colluvial/eolian deposits that are interpreted to closely post-date surface-faulting events.

Figure 1-14. Photograph of spring deposits on footwall of central strand of the Hubbell Spring fault zone. Note sharp base and top of this <10-cm thick deposit of micritic calcium-carbonate cemented sandstone.

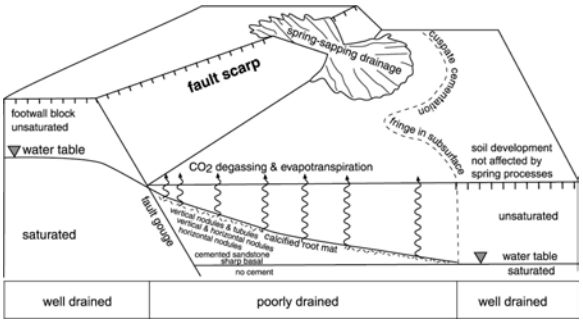

Figure 1-15. Conceptual diagram of spring-deposit formation and the spatial and hydrologic relationship to soil development in fault blocks with identical alluvium on both sides. As calcium-carbonate saturated water drains from the uplifted block to the downthrown block, calcium-carbonate is precipitated in a narrow wedge (Love and Whitworth, 2001). Hachures indicate soils.

Continue driving east on SP-60. **1.0**

13.0 Whaleback feature at 9:00 is deformed piedmont conglomerate and underlying Permian sandstone on footwall of eastern strand of the Hubbell Spring fault zone (Fig. 1-16). The northern Hubbell bench is deeply embayed by streams originating from the Manzanita Mountains. The escarpment formed by the central Hubbell Spring fault has been eroded to the east by as much as 640 m by Cañada Colorada, resulting in the development of a sinuosity value (Bull, 1984) of 3.7 (Karlstrom et al., 1997). **0.3**

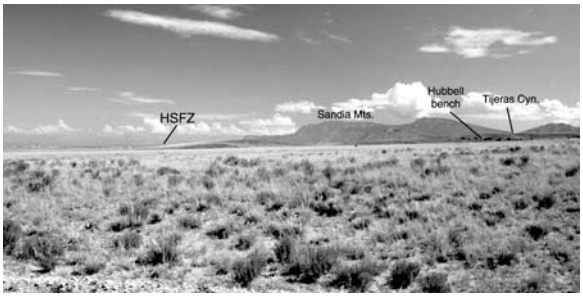

Figure 1-16. Photograph look north of trace of central strand of Hubbell Spring fault zone, marked by low hill in the middle ground. Sandia Mountains in distance.

13.3 Cross cattle guard. Road to southeast is SP-603. Continue straight and ascend deposits of colluvium, alluvium, and spring deposits along edge of northern Hubbell bench. **0.3**

13.6 Contact between east-tilted Yeso Fm (Permian) overlain by 15-20 m of well-cemented, clast- and matrix-supported, limestone-bearing conglomerate (Fig. 1-17). This conglomerate is well cemented by fine-grained sparry calcite. The gorge to the south is Hell Canyon Wash. Note older surfaces above piedmont-plain south of Hell Canyon. **0.3**

13.9 Limestone cobbles and boulders next to road are completely covered with thick calcium-carbonate. Ascend onto the Cañada Colorada surface, a gently west-sloping constructional surface of probable Pliocene age formed on a wedge of well-cemented conglomerate and sandstone derived from the front of the Manzanita Mountains. White pebble gravel on road to the east is composed mostly of hard petrocalcic peds of the Cañada Colorada soil. Mouth of Hell Canyon at 12:00. Mouth of Cañada Colorada at 10:00. Note that the banded rocks (limestone of the Pennsylvanian Madera Group), which form the topographic divide of the Manzanita Mountains, are dropped down-to-the-west by a series of

faults at 10:00. Buildings to the north are research facilities of Sandia National Laboratories. The northern Manzanita Mountains are deeply embayed and have a range front sinuosity of about 6. The shiny metallic structures on the lone hill, just west of the mountain front, are the Starfire Optical Observatory, built as part of the Strategic Defense Initiative of the 1980s. This structure sits on an inselberg of Proterozoic schist on the footwall of the "range-bounding" Coyote fault. The range is deeply embayed and the Coyote fault only marks the range-front at the toes of major spur ridges. This degree of embayment suggests that the Manzanita Mountains are tectonically inactive. Scattered inliers of Pennsylvanian limestone are locally exposed on the piedmont-slope between the Coyote and Tijeras fault zones.

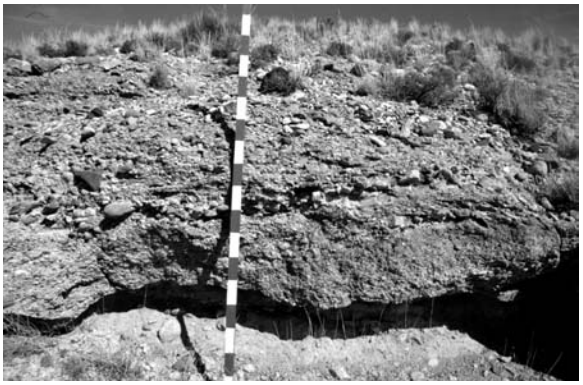

Figure 1-17. Photograph of well cemented, clast-supported, locally derived piedmont deposits exposed on the northern Hubbell bench. Gravel is mostly rounded limestone and reddish-brown sandstone with minor granitic and metamorphic clasts.

The Tijeras fault is a northeast-trending fault that has a long and complicated history of recurrent movement ranging from Quaternary to Proterozoic in age (Connolly et al., 1982; Kelson et al., 1999; Abbott et al., 1995). The southwest projection of this feature into the Albuquerque Basin nearly coincides with the zone of Plio-Pleistocene basalt fields on the Llano de Albuquerque and generally corresponds to a shift in regional patterns of stratal tilt. These features were used as evidence to suggest that the Tijeras fault zone continued across the Albuquerque Basin as an accommodation zone (Russell and Snelson, 1994). The Tijeras accommodation zone was considered to represent a zone of weakness that resulted in accommodating stratal tilts of the Calabacillas and Belen sub-basins (northern Albuquerque and Belen basins) in a scissors fault manner. Geologic mapping and aeromagnetic studies (Maldonado et al., 1999; Grauch, 2001) indicate that the Tijeras fault zone appears to merge into, and probably connects with or is cut by, faults of the Hubbell Spring fault zone, instead of continuing across the basin as a discrete, sub-basin bounding structure as suggested by Russell and Snelson (1994). The east-tilted dip-slope of the Sandia Mountains are clearly visible to the north. **0.5**

14.4 Note lower, inset surfaces associated with Cañada Colorada to the north. **0.6**

15.0 Gate to north pasture. Junipers are present at this elevation (~5680 ft). **0.6**

15.6 Turn right (south) onto two-track road towards windmill at 11:00. **0.4**

16.0 Bottom of Memorial Draw. **0.2**

16.2 **STOP 1-3. Northern Hubbell bench.** Park near windmill. *Mount Washington 7.5' quadrangle, GPS: NAD 83, UTM Zone 013 S, N: 3,862,250 m; E: 363,665 m.*

At this stop, we compare the deep dissection of the northern Hubbell bench and the broad, feature-poor landscape of the Llano de Manzano. Piedmont deposits of the eastern margin are locally derived and form typical proximal, medial, and distal facies. They commonly consist of subangular limestone, metamorphic, sandstone, and granitic pebbles and cobbles; boulders are common near the mountain front. Eolian sand sheets are common on medial and distal portions of the piedmont. The eastern margin of the basin can be divided into three geomorphic domains: 1) incised axial and tributary river valley; 2) weakly dissected piedmont; 3) deeply dissected piedmont (Fig. 1-18 and 1-19).

The front of the Manzanita Mts is deeply embayed and contains exposed or shallowly buried Pennsylvanian-Triassic rocks on the hanging wall of the range-bounding fault. Pleistocene-age fault scarps are recognized on the intrabasinal Hubbell Spring fault zone. In contrast, the front of the northern Manzano Mts is rather linear and contains Pleistocene fault scarps near the mountain front. South of the northern Hubbell bench, a well drilled about 3.7 km west of the mountain front on the Bosque Peak quadrangle (Bonita Land and Livestock well, Karlstrom et al., 1999) encountered deposits of the Santa Fe Group to at least 186 m bls. Cuttings from this well indicated conglomeratic deposits extend to about 64 m and overlie muddy sandstone to the bottom of the hole.

The broad west-sloping piedmont is the Cañada Colorada surface, which is preserved on the footwall of the eastern Hubbell Spring fault zone. This surface lies within the deeply dissected piedmont domain. I contrast the Llano de Manzano is only slightly dissected and rift-border drainages deposit sediment

onto the abandoned piedmont slope and basin-plain of this geomorphic surface complex (Fig. 1-19). A Pliocene age for the Cañada Colorada surface is suggested by geomorphic criterion: it lies about 52 m above the plain of the Llano de Manzano, is deeply embayed, having a range-front sinuosity value of 3.7, and contains a 2 m thick petrocalcic soil that has affinities to Stage V carbonate morphologic development. Soils in a pit (MW10S) about 30 m north of the windmill are more than 2.2 m in thickness and contain Stage III+ to V(?) pedogenic carbonate morphology (Fig. 1-20). Another trench excavated about 2.7 km to the east (MW15) exhibits a similar soil that is over 2.1 m thick.

Driller's notes from the nearby windmill (RWP-27, range water project) indicate the presence of about 20 m of conglomerate over reddish-brown shale to 91 m below land surface. The upper 20 m is correlative to the older, well cemented piedmont conglomerate and sandstone of the Santa Fe Group that forms a thin cap on the northern Hubbell bench. These deposits are well cemented and are Pliocene, and perhaps Miocene in age. The age of this deposit is not well constrained but is older than the early Pleistocene deposits on the hanging walls of the central and eastern Hubbell Spring fault zone.

Longitudinal profiles of paleo-stream positions on the Cañada Colorada surface tend to diverge towards the basin. This basinward divergence results in the development of flights of inset deposits and suggests that streams are progressively entrenching into the northern Hubbell bench, presumably in response to base-level adjustments imposed by activity on the many downstream strands of the Hubbell Spring fault zone.

In contrast, the Llano de Manzano is a low-relief basin-floor and piedmont slope with little constructional topography, except locally along intrabasinal fault scarps. With the exception of Tijeras, Hell Canyon, and Abo Arroyos, the largest drainages of the eastern margin, all other drainages of the mountain front are not integrated with the Rio Grande, but instead have their base level set by the Llano de Manzano (Fig. 1-21). Thus, deposits of these smaller, non-integrated drainages are nearly indistinguishable from the underlying strata. The upper part of the basin-fill succession does contain soils that could be used to discriminate the boundary between basin-fill and younger deposition; however, exposures are not sufficient to do this on a regional basis. Also the selection of stratigraphically lower soils to define the end of Santa Fe Group deposition posses considerable problems in correlation across the basin. Much of the deposition on this broad basin-plain/piedmont-slope occurred after development of the Rio Grande Valley. Late Pleistocene and Holocene deposits can be differentiated on the Llano de Manzano by the relatively weak soil development and incision into older deposits that have more strongly developed soils.

Intrabasinal faulting also creates local conditions where suites of inset terrace deposits on the footwall become part of a soil-bounded aggradational succession on the hanging wall. From a practical standpoint, inclusion of deposits with the stratigraphically highest, moderately developed soils is easier to differentiate and is less ambiguous that interpreting lower, poorly dated, soil-bounded unconformities in the section.

Following a number of models of rift-sedimentation (see among others, Gawthorpe and Leeder, 2000; Mack and Seager, 1990; Leeder and Jackson, 1993; Leeder and Gawthorpe, 1987; Blair and Bilodeau, 1988; Dart et al., 1995), we propose that deposition along the eastern margin of the basin is strongly controlled by the activity of basin-margin and intrabasinal faults. The activity of these faults strongly influences the location of the axial-river (ancestral Rio Grande) and interfingering piedmont deposits derived from the Manzanita and Manzano Mts. During basinward migration of the rift-border structure, portions of the former piedmont-slope and basin-floor are uplifted. Younger deposits bypass this footwall block, which becomes a local stratigraphic top (Fig. 1-22). Smaller drainages that are not integrated with the axial-river tend to have their base level set by these abandoned surfaces. Intrabasinal faulting also tends to create local fault wedges. Many of these wedges can be observed near the constructional tops of the basin-fill succession; however, these wedges can also be recognized in the late Miocene (see map of Connell, 1998).

Retrace route back to SP-60. **0.6**

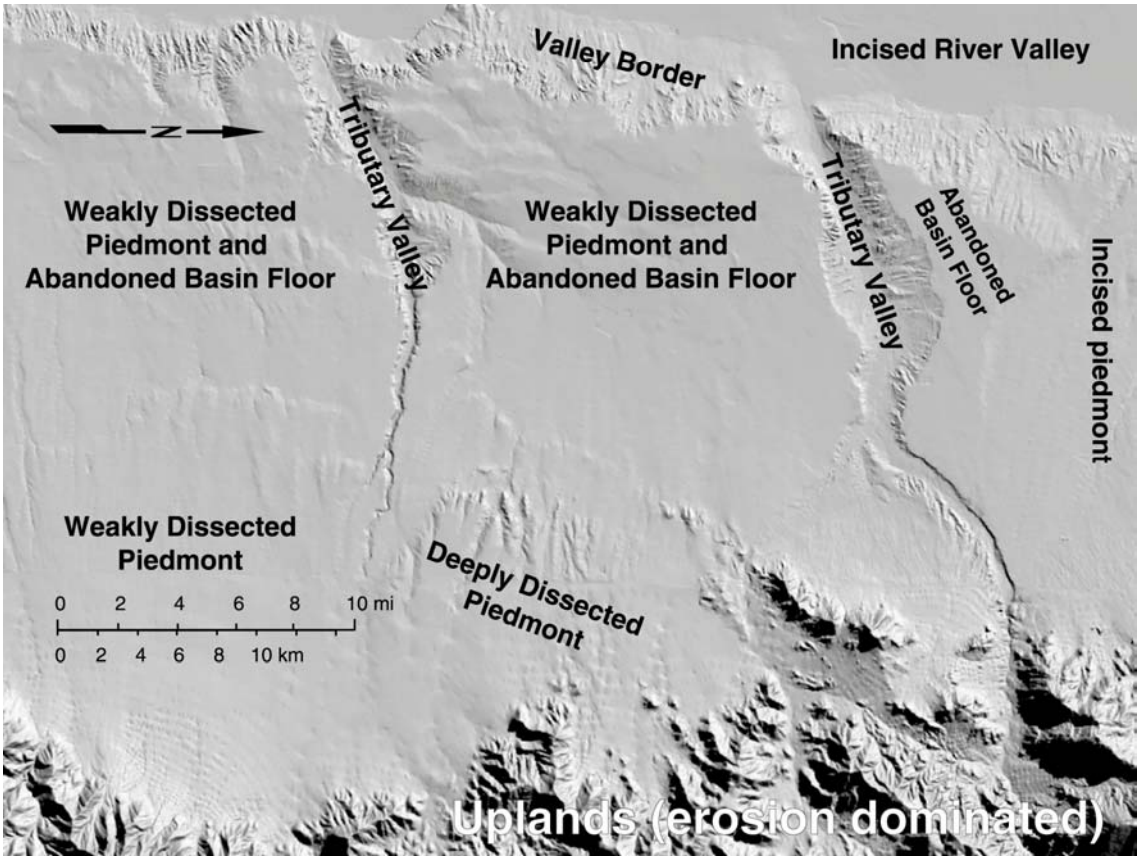

Figure 1-18. Shaded-relief map illustrating variations in mountain-front morphology and piedmont dissection where streams that are not integrated with the Rio Grande and its entrenched tributaries deposit sediment across the low-relief slope of the Llano de Manzano.

Figure 1-19. View of Llano de Manzano south of northern Hubbell bench, illustrating deposition of range-front alluvial fans that prograded over the low-relief, feature-challenged slope of the Llano de Manzano.

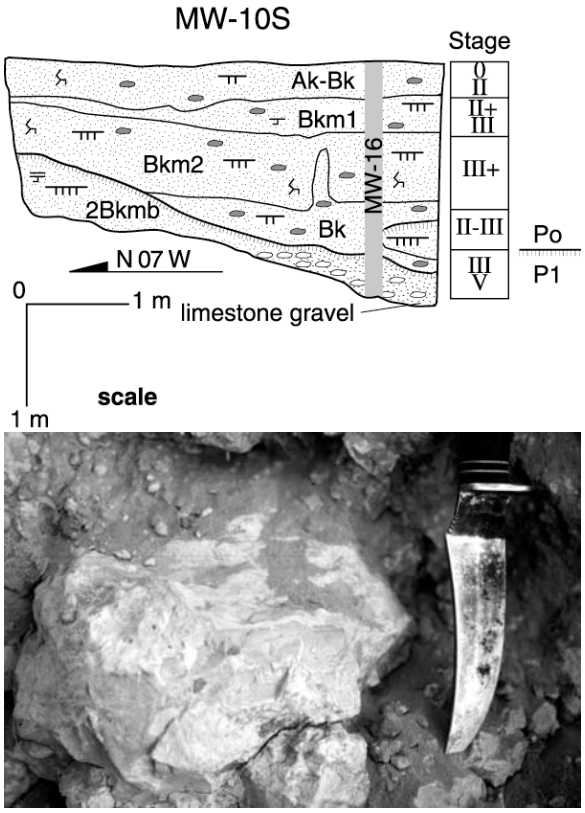

Figure 1-20. Top: Log of soil pit in Cañada Colorado surface. Ticks indicate pedogenic carbonate morphology of each horizon (e.g., single tick= Stage I, double tick=Stage II, triple tick=Stage III). Bottom: Photograph of extremely hard carbonate peds from MW-10S soil pit. Po and P1 denote older and younger soils, respectively.

16.8 Turn right onto SP-60. **1.6**

18.4 To your left is a clear view of down-to-the-west normal faulting within the Manzanita Mountains drops the banded limestone of the Madera Group towards the mountain front. **0.2**

18.6 Turn right (south) onto SP-604. **0.3**

18.9 Descend Cañada Colorada surface into Hell Canyon valley. Note buildings and abandoned mine workings to left on face of Manzanita Mountains. **0.1**

19.0 Descend riser onto middle Pleistocene terrace of Hell Canyon. **0.2**

19.2 The short red pipe about 20 m east of road is the upper East Side Monitoring Well. This well encountered about 21 m of limestone-bearing conglomerate that overlies over 75 m of red clay and sand with limestone layers near the bottom of the hole (at 88 m bls). Groundwater is at about 34 m bls. About 2.9 km to the northeast, just west of the mountain front, a driller's log of a windmill (RWP29) indicates about 21-32 m of gravel over probably Pennsylvanian or Permian rocks. Other monitoring wells drilled on the northern Hubbell bench indicate the presence of about 25-42 m of limestone-bearing gravel correlated to the piedmont deposits of the Santa Fe Group. These conglomerates overlie dark red shale and sandstone of the Permo-Triassic succession. Soil pit (MW8S) just south of road indicates that this deposit contains a soil with Stage III pedogenic carbonate morphology (Fig. 1-23). **0.1**

19.3 Descend riser to Holocene valley of Hells Canyon Wash. Guadalupe Peak at 12:00 with Pennsylvanian limestone nonconformably overlying Ojito granite (Karlstrom et al., 2000). **0.1**

19.4 Crossing modern channel of Hell Canyon Wash. A low (<2 m high) terrace contains charcoal that was dated at 1220±60 yr BP (Beta 106204; dendrochronologically calibrated to 675-975 yr AD, ±2σ). **0.1**

19.5 Note toes of mountain-front fans to your left. Canon de los Seis to southeast. Topography is slightly undulatory and buried soils are common. Exposures of gas line to south indicate an extensive, but locally discontinuous cover of grus-dominated sand with Stage I and II pedogenic carbonate development, overlying moderately developed calcic soil with Stage II to III carbonate morphology. **1.1**

20.6 Note large cobbles and boulders in deposits. **0.2**

20.8 Descend riser onto terrace of Canon de los Seis. **0.2**

21.0 Arroyo exposures of late Quaternary cut and fill terrace sequences. Windmill (RWP-10) to left. **0.1**

21.1 Bear right and head south along fence. **0.6**

21.7 Turn right onto SP-59. **0.2**

21.9 Cross gas pipeline. **0.2**

22.1 Descend low riser into younger grus-dominated alluvium of Cañon de los Seis. **1.8**

23.9 Limestone boulders along edge of Sanchez Canyon, a tributary to Hell Canyon. Suite of inset terrace deposits of Hell Canyon to north. **0.9**

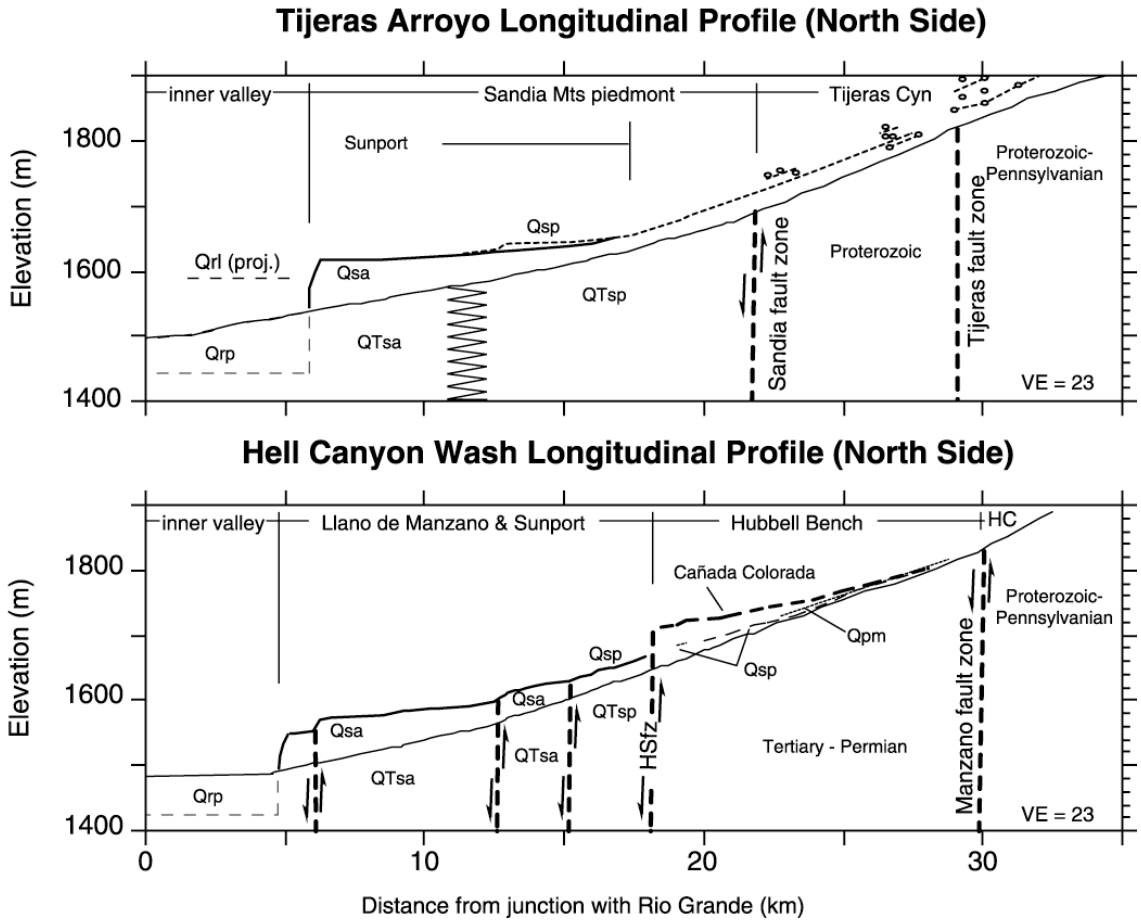

Figure 1-21. Longitudinal profiles of major tributary drainages to the Rio Grande. Top: Tijeras Arroyo, which enters the basin at the junction of the Manzanita and Sandia Mountains. Subsurface work (Hawley and Hasse, 1992; Hawley et al., 1995; Hawley, 1996; Connell et al., 1998) indicate the presence of a number of intrabasinal faults west of the range-bounding Sandia fault. These faults, however, do not significantly influence development of piedmont-slope surfaces. Bottom: Longitudinal profile of Hell Canyon Wash. Intrabasinal faulting by the Hubbell Spring fault zone significantly influences late-stage sedimentation of the Santa Fe Group and the development of piedmont surfaces. Uplift of footwall blocks resulted in the preservation of flights of piedmont and valley-fill units that become nearly indistinguishable from the aggradational succession on the hanging wall.

24.8 Cut in low, middle Pleistocene terrace across tributary to north contains a stack of calcic soils (MW1S), illustrating a succession of soils containing I+ (25 cm thick), and III+ (90-125 cm thick) pedogenic carbonate morphology. A gas line excavated across the piedmont exposed much of the piedmont-slope south of Hell Canyon Wash. This trench contained a strongly developed soil with Stage III carbonate morphology and clay-rich Bt horizons. Younger grus-dominated sands overlie this soil. **0.2**

25.0 Cross cattle guard. **0.2**

25.2 Cross over interfluve between Ojo de la Cabra and Hell Canyon drainages. **0.5**

25.7 Turn to right and stay on SP-59. Descend onto terrace tread. **0.5**

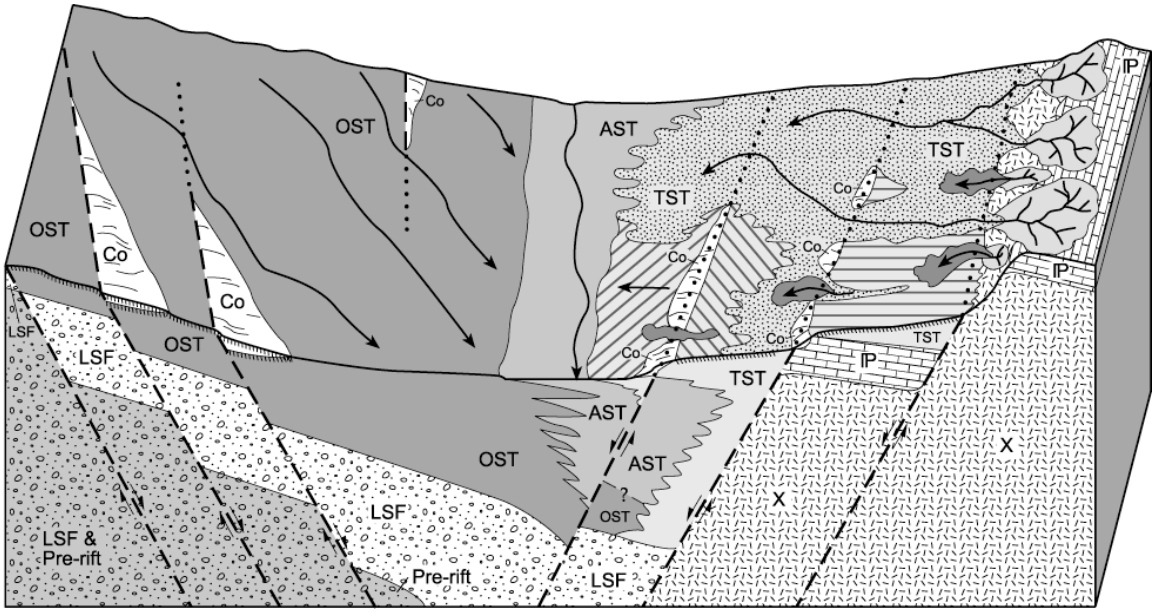

Figure 1-22. Conceptual block diagram, illustrating regional patterns of Santa Fe Group sedimentation (inspired after Gawthorpe and Leeder, 2000). Deposition along the footwall of the basin (transverse and axial systems tracts, TST and OST, respectively) are influenced by the location and activity of intrabasinal normal faults. In particular, basinward migration of the eastern rift-border structure results in the preservation of a number of geomorphic surfaces on the footwalls of intrabasinal faults. Depending on the size and lithology of the footwall drainages, piedmont deposition may be integrated with the axial river (AST) or will grade to local base levels along the eastern margin. Stratigraphic (or syntectonic) wedges are locally preserved along exposed fault scarps (co).

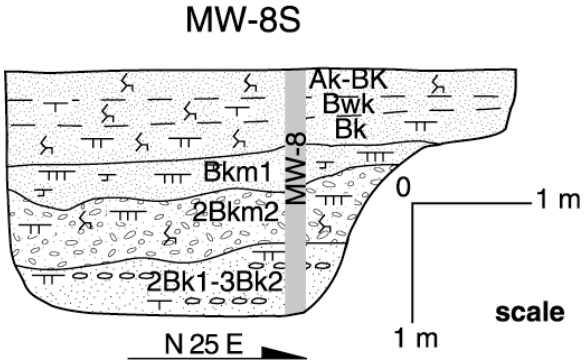

Figure 1-23. Log of soil pit on inset middle(?) Pleistocene terrace deposit of Hell Canyon Wash. Ticks indicate pedogenic carbonate morphology of each horizon (e.g., single tick= Stage I, double tick=Stage II, triple tick=Stage III).

26.2 Descend riser. Junipers on lower tread surfaces. **STOP 1-4**. **Inset terrace deposits of Hell Canyon Wash**. *Hubbell Spring 7.5' quadrangle, GPS: NAD 83, UTM Zone 013 S, N: 3,861,415 m; E: 362,310 m.*

This stop is an overview of the suite of inset terrace deposits associated with Hell Canyon Wash. Upstream and to the east, Hell Canyon Wash is a rather broad valley. West of here is the canyon of Hell Canyon Wash, which entrenched into the upper Santa Fe Group basin fill during early(?) or middle Pleistocene time. To the south, drainages developed on the footwall of the Manzano Mountains are not integrated with Hell Canyon Wash or the Rio Grande. These drainages terminate on abandoned, early Pleistocene basin-plain and piedmont-slope surfaces, which constitute base level control for such streams. At this stop four terrace levels are visible above the modern channel. The lowest terrace is 2.5-3 m above the modern channel and functioned as the floodplain/valley floor during the 20th Century and probably consists of Holocene fill. The second level is discontinuous and is ~6 m above the modern channel. This small local terrace deposit is cut into an adjacent 9-m high terrace level and could represent local (autocyclic?) variations in arroyo cutting and filling, rather than being related to tectonically or climatically driven changes in the landscape. However, other 6-m high terraces are present downstream. An extensive terrace is 9 m above the modern channel here. This terrace deposit is not preserved down stream. The next highest terrace is 10-11 m above the modern channel. This unit becomes a broad, extensive terrace deposit downstream and is preserved on both sides of Hell Canyon Wash. The highest terrace is 12-13 m above the modern channel and locally forms a broad rounded drainage-divide that SP-59 follows. To the west is an older surface that is 27 m above the modern channel. The problem with correlating terraces in this geomorphic setting is that they become discontinuous downstream and are buried by

eolian and alluvial sediments upstream. Their age, climate and tectonic significance remain elusive.
Turn around and head back to MM 25.7. **0.2**

26.4 Turn right (west) onto Hell Canyon Road (SP-625), heading west on interfluve of Ojo de la Cabra (Goat Spring) drainage. **0.5**

26.9 Cross cattle guard. **0.6**

27.5 Descend into Ojo de la Cabra drainage. **0.1**

27.6 Road crosses terrace remnant, which merges into the valley floor upstream and is buried by piedmont alluvium farther east. **0.1**

27.7 Road parallels Holocene terrace to south that contains charcoal and snails. **0.2**

27.9 Notice the presence of phreatophytes (e.g., reeds and rushes) as you pass the spring of Ojo de la Cabra (Goat Spring). Note the abundance of Mesquite and Creosote down stream. We are near the northern limit of Creosote, which defines the northern limit of Chihuahuan Desert vegetation. **0.2**

28.1 Confluence between Ojo de la Cabra drainage with Hell Canyon Wash. Two discontinuous levels of terraces are present here. Piedmont deposits consist of sandstone with interbedded clast-supported conglomerate composed mostly of limestone with subordinate metamorphic and minor reddish-brown sandstone cobbles and boulders. **0.4**

28.5 Note terrace deposits midway up margins of Hell Canyon Wash. **0.5**

29.0 Buried paleocanyon on north side of drainage contains about 10-15 m of bouldery piedmont sediments. **0.2**

29.2 Arroyo terrace deposit to north is inset against upper Santa Fe Group. **0.1**

29.3 Hell Canyon Wash broadens, presumably because of the presence of weakly cemented fluvial deposits of the ancestral Rio Grande below just level of valley floor. Drainages developed in ancestral Rio Grande deposits commonly form broad tributary valleys, whereas, tributary drainages incised into the better cemented piedmont deposits commonly contain narrower and steeper-walled valleys. **0.4**

29.7 Paleo-canyon backfill (s) exposed on north rim of Hell Canyon Wash. Historic gravel bars on valley floor may have been deposited during flood in the 1920s(?). There are anecdotal accounts of a flood in Hell Canyon that reached the Rio Grande in the 1920s, however, the extent of this flood has not been independently verified. **0.6**

30.3 To your right at valley floor level are well cemented, gently east-tilted exposures of early Pleistocene pumice-bearing ancestral Rio Grande deposits. **0.1**

30.4 Cross cattle guard. **0.3**

30.7 **STOP 1-5. Hell Canyon Wash**. *Hubbell Spring 7.5' quadrangle, GPS: NAD 83, UTM Zone 013 S, N: 3,862,700 m; E: 355,420 m.*

A stratigraphic section measured along the southern margin of the arroyo is on the footwall of an intrabasinal fault. The lower part of this section contains deposits of the ancestral Rio Grande that contain locally abundant pumice pebbles. A pumice was dated using the $^{40}Ar/^{39}Ar$ method at 1.71 Ma. Geochemistry of this dated pebble indicates that it is chemically similar to the Bandelier Tuff (N. Dunbar, 2001, personal commun.). However, its age is slightly older than the lower Bandelier and may be related to the pre-caldera San Diego Canyon ignimbrite. About half-way up the slope is a cross-bedded pumice-bearing pebble conglomerate that is well cemented with sparry calcite and forms elongate concretions (Fig. 1-24). The orientations of such elongate concretions are bi-directional indicators of paleo-groundwater flow (Mozley and Davis, 1996). Assuming that paleo-groundwater flow directions roughly mimic the present southward course of the Rio Grande, the orientations of these elongate concretions are south-southeast. Paleocurrent orientations determined from cross bedding are south-southwest, but similar to the paleo-groundwater flow indicators. A succession of fine- to medium-grained sand with scattered concretionary sandstone and rhizoconcretionary intervals is typically present between the underlying fluvial and overlying piedmont deposits. Cementation of the underlying fluvial succession is also common near the boundary (laterally or vertically) with eastern-margin piedmont deposits. Fluvial and eolian-dominated deposits interfinger with, and are overlain by, locally derived piedmont deposits of the Manzano Mts.

The top of the section contains a strongly developed soil with Stage IV pedogenic carbonate morphology and a strongly developed stone pavement. This surface is a remnant of the footwall of a strand of the Hubbell Spring fault zone. Later piedmont deposits bypassed this remnant to the north and south of Hell Canyon. Deposits of these later piedmont systems are only slightly offset by this fault strand, but are displaced more by other strands to the west. The tops of limestone pebbles on this constructional surface are commonly flattened, probably by the dissolution of carbonate. The undersides of these clasts are quite deeply pitted and have a pendant morphology caused by the dissolution of calcite. Later re-precipitation of white micritic carbonate indicates deposition after an earlier stage of dissolution. These cements are quite different than the sparry, phreatic calcite exposed below in the fluvial deposits of the ancestral Rio Grande (Fig. 1-25 and 1-26).

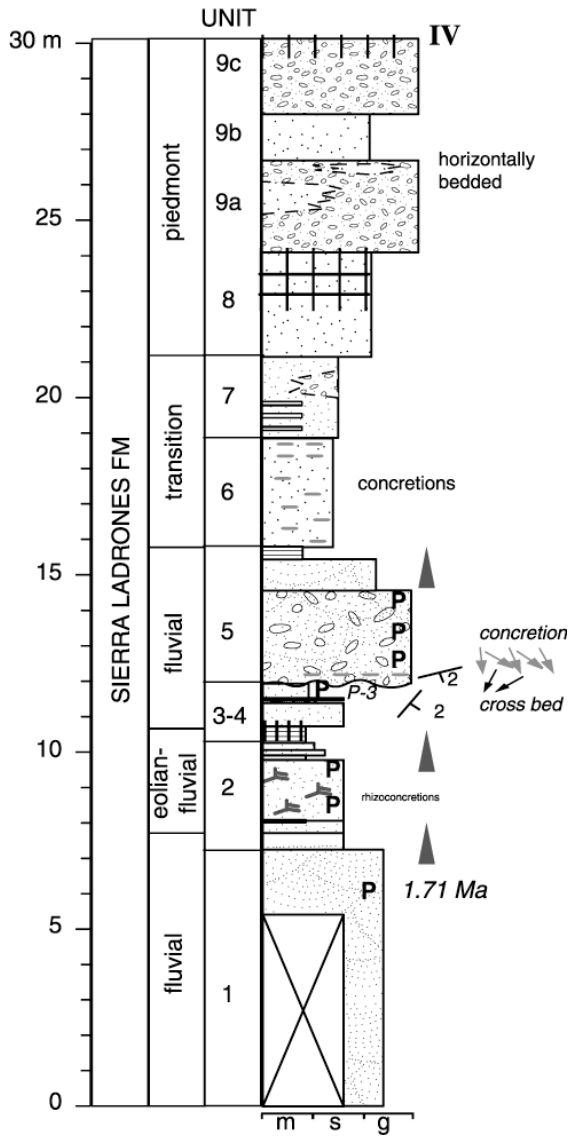

Figure 1-24. Stratigraphic section of Hell Canyon Central Section measured along southern margin of Hell Canyon. This marks the approximate eastern limit of exposure of pumice-bearing fluvial deposits of the ancestral Rio Grande, which become buried to the east. Hachures denote soils. Roman numerals indicate pedogenic carbonate morphologic stage.

Comparisons of surface and available subsurface stratigraphic data indicate the development of a westard-prograding wedge of ancestral Rio Grande and eastern-margin piedmont deposits (Fig. 1-27). This westward progradation of the ancestral Rio Grande would result in onlap onto deposits of the Arroyo Ojito Fm (the western oblique fluvial system). The top of the Arroyo Ojito Fm is defined by the Llano de Albuquerque surface, which is late Pliocene in age (see discussions in Day 2 road log).

Figure 1-25. Photograph looking to the east at well cemented extrabasinal, cross bedded sandstone and rounded conglomerate of the ancestral Rio Grande deposits of the Sierra Ladrones Fm. The banded appearance is the result of southerly oriented sandstone concretions indicating a southerly direction of paleo-groundwater flow. Scale is 1.5 m high.

Thus, this westward progradation of the Rio Grande would result in the development of an unconformity of increasing temporal magnitude to the west (see Fig. 1-6). The nature of this contact will be explored on Day 2. This westward progradation of the ancestral Rio Grande and piedmont deposits is recognized throughout much of the basin (see Connell et al., 1995; Cather et al., 2000; Smith et al., 2001 for examples) and may be responsible for the present position of the Rio Grande Valley, prior to 0.7-1.2 Ma entrenchment. This relationship may also explain why deposits of the ancestral Rio Grande in the Albuquerque area are rather sparse west of the Rio Grande Valley.

Geologic studies of the Isleta Reservation do not support the presence of an eastern buttress unconformity between early Pleistocene fluvial deposits of the ancestral Rio Grande and older basin fill. Figure 1-28 is a conceptual model showing interpreted differences in bounding unconformities and stratal geometries one might expect between aggrading basin fill and incised river valley deposition.

Continue driving west on SP-625. **0.5**

31.2 Ancestral Rio Grande deposits low in canyon walls, east of a strand of the Hubbell Spring fault zone. These deposits commonly form “flat irons” (Gerson, 1982) that are separated from the modern valley border slopes. These are probably the result of differential permeability and runoff contrasts between the more permeable ancestral Rio Grande deposits and the less permeable piedmont alluvium. North side of Hell Canyon Wash widens. Badlands contain interfingering distal piedmont and ancestral Rio Grande deposits. **0.1**

31.3 Pass connecting road to SP-624. Bear left. **0.2**

31.5 Road to right across dam leads to exposures of interfingering transition between piedmont and fluvial deposits. **0.2**

31.7 Valley broadens and interfingering piedmont deposits become thinner. **0.4**

32.1 High terrace deposits across valley to your right. Piedmont deposits above are generally less than 2 m thick and cap both edges of Hell Canyon Wash. **0.4**

32.5 Low terrace deposit from Memorial Draw, to north, which follows the McCormick Ranch fault. **0.5**

33.0 Cross road from northeast. Large boulders of upper Bandelier Tuff found to south (Fig 1-29). Note terrace, about 7 m above road, along south side of Hell Canyon Wash. **0.3**

33.3 Terrace deposit continues on south side of Hell Canyon but become more dissected to the west. **1.2**

34.5 Cross trace of Palace-Pipeline fault zone, which displaces the Llano de Manzano by about 18 m on south side of Hell Canyon Wash. Terrace to your left (south) terminates near trace of fault. This terrace is probably middle to late Pleistocene in age. It is not clear whether the fault displaces this terrace to the extent that it is buried below the valley to the west. Rather, this terrace is probably too thick to be offset that much. Capture of new tributaries west of the Palace-Pipeline fault and erosion of the valley margins may provide a better explanation for the lack of terraces to the west. **0.7**

35.2 Cross cattle guard. Exposures at 9:00 and 2:00 contain an ash preliminarily dated at 1.55 Ma and correlated to the Cerro Toledo Rhyolite. Earlier attempts to date this fine-grained ash yielded a range in ages from 1.05-1.6 Ma. **0.6**

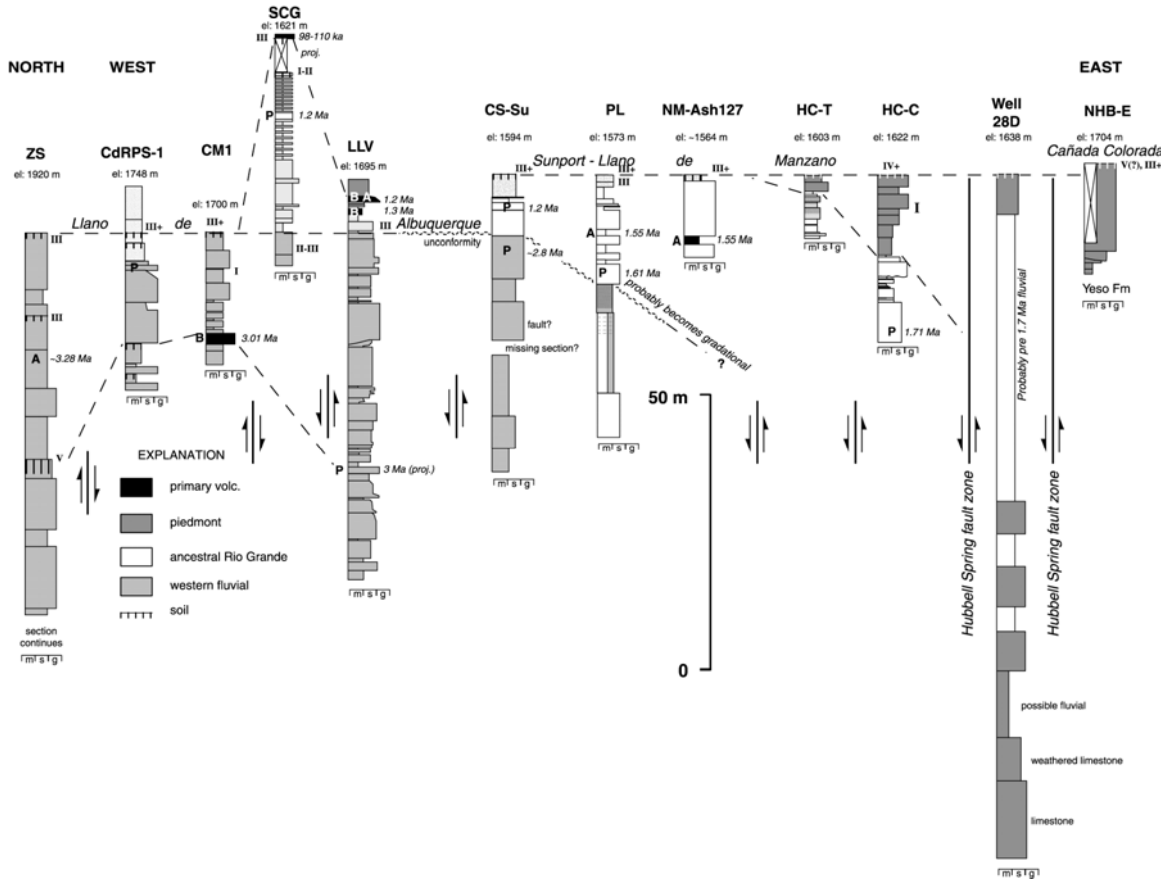

Figure 1-27. Stratigraphic fence across a portion of the Isleta Reservation and Los Lunas volcano, illustrating stratigraphic relationships among upper Santa Fe Group deposits. Horizontal distances are not to scale. See **Plate II** for approximate locations of stratigraphic sections. The Zia fault section (ZS) is about 45 km north of CdRPS-1 and contains the ~3.3 Ma Nomlaki Tuff (Connell et al., 1999). Hachures denote soils. Roman numerals indicate pedogenic carbonate morphologic stage.

Figure 1-26. Photograph of constructional surface at top of stratigraphic section, illustrating a deeply pitted limestone pebble covered with micritic carbonate. The interlocking flat pebbles form a moderately to well developed desert pavement. Limestone pebble tops are commonly flattened and subparallel to the ground surface.

35.8 Turn right (north) towards cattle guard at north end of Hell Canyon Wash. **0.2**

36.0 Cross cattle guard. **0.1**

36.1 Begin pavement, turn north and drive on floodplain of Rio Grande. Bluffs to east contain pumice-bearing ancestral Rio Grande deposits. **0.7**

36.8 White bed at 3:00 is ash dated at 1.55 Ma and correlated to Cerro Toledo Rhyolite. This ash is about 10 m below the Sunport surface. (Fig. 1-30). **0.8**

37.6 Bluffs to east expose fine-grained light-brown sand overlain by gray deposits of the ancestral Rio Grande. This contact descends to the south and is buried at the mouth of Hell Canyon Wash. **0.8**

38.4 Cross cattle guard and turn right onto state highway NM-47. Merge into left lane. **0.4**

38.8 Turn left onto state highway NM-147 towards Isleta Pueblo. Bluff to north is low terrace. **0.2**

39.0 Cross Rio Grande. The concrete structure that spans the river is the Isleta Diversion Dam of the Middle Rio Grande Conservancy District, which diverts water from the Rio Grande to a number of acequias (*ditches*) for irrigation agriculture between of Isleta and San Acacia, New Mexico. Much of this water is returned to the river via a series of drains. **0.3**

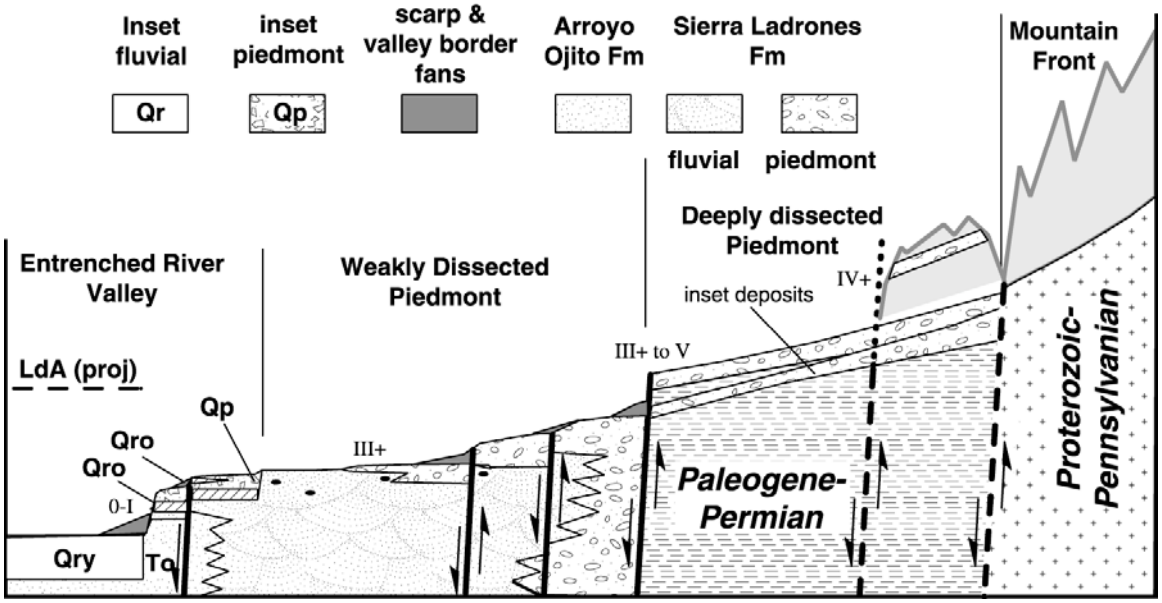

Figure 1-28. Schematic stratigraphic relationships comparing deposition on deeply dissected and weakly dissected piedmonts and the entrenched river valley. Units Qro and Qry denote younger and older inset fluvial deposits.

Figure 1-29. Photograph of boulder of upper Bandelier Tuff within early Pleistocene sand and gravel of the ancestral Rio Grande deposits of the Sierra Ladrones Fm. This boulder is exposed in a gully just south of Hell Canyon Wash.

Figure 1-30. Photograph of white fluvially reworked ash of Cerro Toledo Rhyolite exposed along eastern margin of Rio Grande Valley. This ash lies about 30 m above the local base of early Pleistocene sand and gravel of the ancestral Rio Grande deposits of the Sierra Ladrones Fm.

39.3 Turn left to Isleta Pueblo (pop: 4409). The Pueblo of Isleta (Spanish for *island*) was built on a slightly elevated fluvial-terrace deposit of the Rio Grande. A basalt flow crops out on the northern side of the "island of Isleta." The original pueblo was located on the site of the present pueblo when Coronado visited the area in 1540.The Spanish established the Mission of San Antonio de Isleta by 1613. Plains-Indian raids caused the Pueblo Indians living east of the Manzano Mountains to move to Isleta around 1675. The Isleta Pueblo did not actively participate in the Pueblo Revolt against the Spanish in 1680 and became a refuge for Spanish settlers. In spite of this Governor Otermin captured the pueblo in 1681 and took 400 to 500 prisoners with him to El Paso where they settled at Ysleta del Sur. The remaining population abandoned the Pueblo of Isleta and fled to Hopi country. They returned in 1716, brining their Hopi relatives with them. The present Pueblo was built in 1709 by scattered Tigua families. Most of the Hopi later returned to Arizona, but have retained their ties with Isleta. Reservations of Acoma and Laguna migrated to Isleta in the early 1800s because of drought and religious differences at their home pueblos. Thus, Isleta has incorporated a variety of pueblo people (Taken from Connolly, Woodward, and Hawley, 1982, p. 29). **0.1**

39.4 Bear right at cylindrical cement water tank and continue west to plaza. **0.1**

39.5 Cross plaza and church at Isleta. **0.1**

39.6 Turn right (north) at intersection west of plaza. **0.2**

39.8 Turn left onto state Highway NM-147. **0.7**

40.5 Cross railroad tracks and immediately turn left onto NM-314. **0.3**

40.8 Turn right onto Tribal Road TR-74. Drive slow and watch for speed bumps. **0.2**

41.0 Turn left onto NM-45 at stop sign, then make a quick right onto NM-317 towards junction with I-25. **0.8**

41.8 Ascend onto Los Duranes Fm, a late-middle Pleistocene fluvial deposit of the ancestral Rio Grande that is inset against Santa Fe Group basin fill. The top of this deposit was named the Segundo Alto surface by Lambert (1968). The age of the top is constrained by the 98-110 ka Cat Hills flows, which overlies the Los Duranes Fm (Fig. 1-31). About 25 km to north in NW Albuquerque, tongues of the 156±20 ka (U/Th date from Peate et al., 1996) Albuquerque volcanoes are interbedded near the top of the Los Duranes Fm. These constraints indicate that deposition of the Los Duranes Fm ceased between 98-156 ka. A prominent tributary terrace deposit in Socorro Canyon, about 105 km to the south near Socorro, New Mexico, has been dated using cosmogenic ^{36}Cl dating methods, indicates a cessation in deposition at 122±18 ka (Ayarbe, 2000). Correlations to this better-dated deposit have not been made, but suggest that the development of the Segundo alto terrace tread surface may be near this vintage. **0.3**

42.1 Cross I-25 overpass. Continue west. **0.2**

42.3 Cross cattle guard, heading west on Segundo alto surface. Pavement ends. Black hill to right (north) is the 2.78 Ma Isleta volcano (Maldonado et al., 1999). **0.2**

42.5 Low eastern limit of younger flows of Cat Hills volcanic field, which have been $^{40}Ar/^{39}Ar$ dated between 98-110 ka (Maldonado et al., 1999). **0.8**

Figure 1-31. View, looking west, of late Pleistocene basaltic flows of the Cat Hills volcanic field overlying the Segundo alto surface of the Los Duranes Fm.

43.3 Pass transfer station to your left. The Shell Isleta #2 well was drilled just west of Isleta volcano to the north. **0.7**

44.0 Flows of the late Pleistocene Cat Hills volcanic field to the south. **1.3**

45.3 Cross wash and turn left (southwest) on dirt road. **0.5**

45.8 The prominent hill to south is the Pliocene and early Pleistocene Los Lunas volcano. Volcano intruded deposits of the Arroyo Ojito Fm and Sierra Ladrones Fm. **0.6**

46.4 Pass through locked gate. **0.3**

46.7 Drive on Cat Hills flow 1. **0.4**

47.1 On Arroyo Ojito Fm. **0.2**

47.3 Flow of unit 1 of the Cat Hills basalt field. **0.3**

47.6 Exposures of the Arroyo Ojito Fm. **0.5**

48.1 On flow 1 of Cat Hills field. Excellent view of north side of Los Lunas volcano. **0.2**

48.3 Descend into eroded units of sand and mud exposed in the San Clemente graben. **0.1**

48.4 Cross drainage covered by eolian sandsheets and fine-grained mud and sand dominated deposits that fill the San Clemente graben. **0.4**

48.8 North-trending alignment of vents of the Cat Hills field to the west. **0.5**

49.3 Pass under powerlines. **0.4**

49.7 Bear right at corral and windmill. **0.4**

50.1 Pass Cat Hills basalt flow overlying strongly developed soil on right. **0.1**

50.2 **STOP 1-6.** San Clemente graben and Cat Hills volcanic field. *Dalies 7.5' quadrangle, GPS: NAD 83, UTM Zone 013 S, N: 3,856,670 m; E:332,080 m.*

Deposits within the San Clemente graben are mostly muddy sand and sand of eolian, fluvial, and colluvial origin. These deposits rest on a soil developed on the upper Arroyo Ojito fm (Ceja Mbr) and are overlain by flows of the Cat Hills field (Fig. 1-32). Strongly developed soil with stage III+ carbonate morphology are present at this upper contact. A bed of pumice-bearing pebbly sand is exposed locally in upper part of the San Clemente graben succession (Fig. 1-33). This pebbly sand bed contains pumice that has been chemically correlated to the Bandelier Tuff and yields a $^{40}Ar^{39}Ar$ date of 1.2 Ma, indicating that it is correlated to the upper Bandelier Tuff. These deposits overlie a soil developed on deposits of the Arroyo Ojito Fm. This soil is interpreted to represent a buried correlative of the Llano de Albuquerque soil, which marks the local top of Arroyo Ojito Fm deposition. The presence of Bandelier Tuff suggests that these sandy deposits are part of the ancestral Rio Grande deposits of the Sierra Ladrones Fm and represent the westernmost progradation and temporary spillover of the ancestral Rio Grande into the San Clemente graben during early Pleistocene time (Fig. 1-34).

Turn around and retrace route back to paved road west of I-25. End of day one road log. **8.0**

Figure 1-32. View to west of the 98-110 ka flow of the Cat Hills volcanic field, which overlies a strongly developed soil that exhibits Stage III pedogenic carbonate morphology. This soil is developed on sand and mud of the San Clemente graben, which overlies a soil developed on the Ceja Member of the Arroyo Ojito Fm.

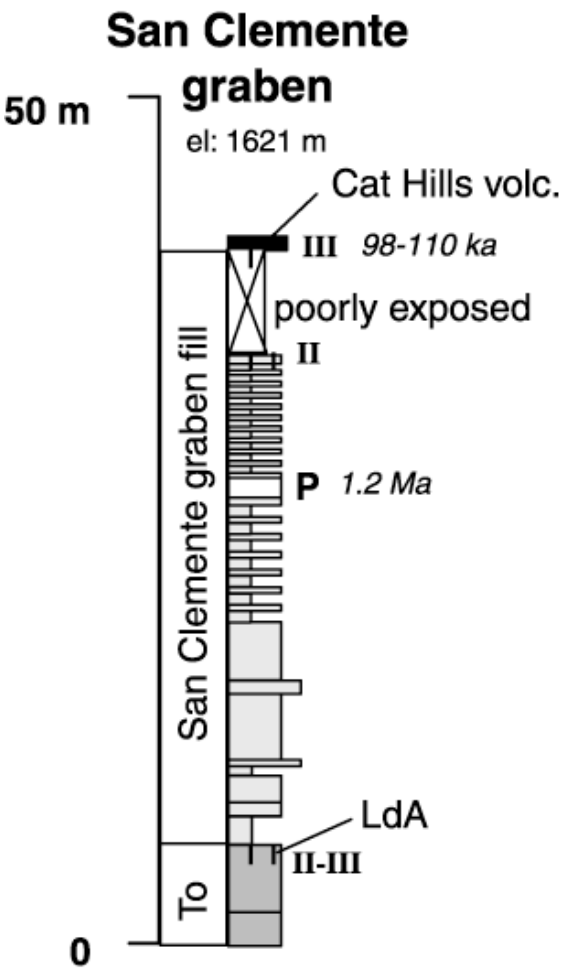

Figure 1-33. Stratigraphic column of San Clemente graben site, illustrating about 40 m of sand and mud overlying a soil developed on deposits assigned to the Ceja Member of the Arroyo Ojito Fm. About 18 m above the basal contact is a bed of sand containing pebbles of fluvially recycled upper Bandelier Tuff (verified by $^{40}Ar/^{39}Ar$ dating and geochemical correlation; W.C., McIntosh, and N. Dunbar, unpubl.). Hachured lines denote soils. Roman numerals indicate pedogenic carbonate morphologic stage.

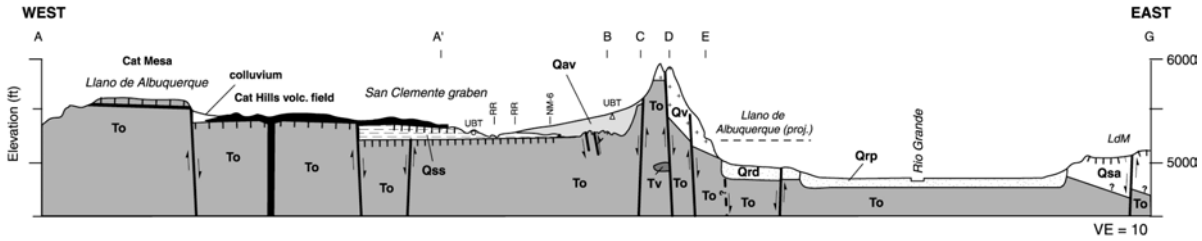

Figure 1-34. Cross section across western edge of basin and Los Lunas volcano. Note that the Llano de Albuquerque is faulted down towards the east and is buried by sediments accumulated in the San Clemente graben, which contains beds of early Pleistocene ancestral Rio Grande deposits in it. The scarp along the eastern edge of Los Lunas volcano is either faulted or is an erosional escarpment formed during entrenchment and subsequent aggradation of the middle Pleistocene Los Duranes Fm. A notch along the eastern flank of Los Lunas volcano marks the edge of an upper flow. Units include the Arroyo Ojito Fm (To), alluvium in San Clemente graben (Qss), ancestral Rio Grande deposits of the Sierra Ladrones Fm (Qsa), alluvium of Los Lunas volcano (Qav), 1.26 Ma trachyandesite of Los Lunas volcano (Qv), older volcanic rocks of Los Lunas volcano (Tv), and inset fluvial deposits of the Los Padillas (Qrp) and Los Duranes (Qrd) fms. Hachured lines denote major geomorphic surfaces, such and the Llano de Albuquerque and Llano de Manzano (LdM). Fallout ash and fluvially recycled pumice of the 1.22 Ma Bandelier Tuff (UBT) is present in units Qss and Qav.